Potential of Adjuvant-induced Lymphangiomas in MIce: Its dvantages as an Animal Model to Study Lymphatic Endothelial Cells

Review

Potential of Adjuvant-induced Lymphangiomas in Mice:
Its Advantages as an Animal Model to Study Lymphatic Endothelial Cells

Taichi Ezaki

Department of Anatomy and Developmental Biology, School of Medicine, Tokyo Women's Medical University, Tokyo, Japan
(Accepted   April 15, 2019)

Studies on the lymphatic system have made remarkable progress with the discovery of lymphatic endothelial cell-specific markers. To discover lymphatic endothelial cell-specific markers, we adopted a Freund's incomplete adjuvant (FIA)-induced lymphangioma model in rodents. The tumor was used as an antigen source of mouse lymphatic endothelium to produce monoclonal antibodies. We obtained LA102, which recognizes lymphatic endothelial cells, but not blood vessel endothelial cells. We found LA102 to be a homolog of mouse CD90.2 (Thy-1.2). Using LA102 and other specific markers for microvessels, including lectins, we have developed 3D-imaging techniques to characterize lymphatic networks to differentiate from blood vessels. This model has also been adopted to investigate the relationship between peritoneal mesothelium and lymphatic endothelium. At three days after FIA injection, simple squamous mesothelial cells became cuboidal and detached from each other to lose their polarity and formed multi layers. Various-sized fat droplets gradually fused with each other, and the fat-storing cells became large fat cells or formed large chimeric follicular structures. At four weeks or later, these cell masses formed tubular structures draining the fat out of the peritoneal cavity. Taking up fat (FIA) droplets, not only podoplanin^{+} mesothelial cells, but also bone marrow-derived macrophages and some interstitial mesenchymal cells were involved in tumorigenicity. We suggest a sequential change from mesothelial to lymphatic endothelial cells via fat-storing lymphangioma cells after FIA stimulation. These phenomena seem to be a defense mechanism, where mesothelial-endothelial transformation might occur via fat incorporation to drain the extrinsic adjuvant oil out of the peritoneal cavity. The significance of FIA-induced lymphangiomas and mesothelial cell diversity might be important for the interrelationship between fat cells and lymphatic endothelial cells.

Key Words: adjuvant, fat, lymphangioma, lymphatic endothelial cell, mesothelial cell

Introduction

Animal tumor models have been used to understand normal cellular life events, because tumors may reflect mirror images of normal cells.[1] There are several tumor models to investigate various phenomena, such as tumor immunity as specific targets for immune reactions,[2-6] thymic nurse cell as a thymic microenvironment in spontaneous thymomas,[7-10] and various tumor angiogenesis.[11-13] In this review, I introduce how an adjuvant-induced lymphangioma rodent model was adopted and demonstrate its potential and use as various experimental strategies.

Corresponding Author: Taichi Ezaki, Department of Anatomy and Developmental Biology, School of Medicine, Tokyo Women's Medical University, 8-1 Kawada-cho, Shinjuku-ku, Tokyo 162-8666, Japan. ezakit@twmu.ac.jp

mAb	artery	arteriole	capillary	venule	vain	lymphatics
B1		▬▬▬▬				
B8			▪▪			
B43			▪ ▬▬▬			
B110			▬▬▬▬▬			
B27	▪···▬▬····			········	▬▬▬▬▬	

Figure 1 Monoclonal antibodies against rat vascular endothelial cells.
The specific reactivity of each monoclonal antibody to various rat microvasculature is expressed as the width range of bars. For example, B1 recognizes endothelial cells of arterioles and capillaries on the arterial side, but not of venous side and venous-type vessels.

As an Antigen Source of Lymphatic Endothelium to Identify the Lymphatic Endothelial Cell Specific Markers

1. Initial studies on vascular endothelial cells

Blood vascular and lymphatic systems play essential roles in local tissue microcirculation. Microvessels have characteristic structures to exhibit their special functions for local microcirculation.[14] For example, arterioles are called as resistance vessels because they constitute the principal component of peripheral resistance to blood flow that regulates the blood pressure. Capillaries, as exchange vessels, may exhibit marked differences in their structures and permeability properties depending on the functional sites in various organs. Capillaries converge to form post-capillary venules (PCVs) or venules of larger size, where cellular or macromolecular passages can take place under both physiological and pathological conditions.[15]

Therefore, we tried to develop strategies to investigate the morphological and functional characteristics of each microvessel. Monoclonal antibodies (mAbs) against rat vascular endothelial cells were produced in mice to characterize and assess the functional properties of the antigens recognized **(Figure 1)**.[16] B1 recognizes rat arteriolar endothelial cells and arterial-side capillaries, but not those of venous-type vessels. Contrarily, B110 recognizes venous-side capillaries, venules including PCVs, some sinuses and small veins, but not any arterial-type vessels **(Figure 2a)**. B8 recognizes endothelial cells in splenic marginal sinuses and certain types of capillaries. B43 recognizes lymph node venules

and hepatic sinusoids. Immunohistochemical identification of microvessels using a panel of these mAbs will provide valuable information for studies on local blood microcirculation.

Despite its critical role in tissue fluid homeostasis, macromolecule or lipid absorption, and immune or malignant cell migration, however, the lymphatic system has not received considerable attention. Lymphatic capillaries have highly permeable structures, and they readily capture fluids, macromolecules, particulate matters, and cells from the connective tissue spaces. However, segmental and functional studies on microvessel networks have not always been successful due to the lacks of reliable techniques to identify these ramifications in the local tissue (Ezaki & Kotani, in this volume[17]). In part this has been due to a lack of specific markers for lymphatic endothelial cells. Therefore, we first produced a mouse mAb, B27, against rat lymphatic endothelium.[18] B27 strongly recognizes endothelial cells of most rat lymphatics, including lacteals, lymphatic capillaries in the diaphragm **(Figure 2b)** at the absorption sites in the peritoneal cavity, collecting lymphatics, and thoracic duct. However, B27 also recognizes the endothelium of some other types of blood vessels. Hence, double immunostaining of B27 should be combined with type IV collagen of basement membrane to discriminate between lymphatic capillaries and blood capillaries on tissue sections **(Figure 2c)**.

2. Requirement for more specific strategies to identify lymphatic endothelial cells

To better understand the lymphatic functions, it is important to discriminate lymphatic vessels from blood vessels and characterize lymphatic endothelial cells under both physiological and pathological conditions.[19-22] Furthermore, various vascular lineage-specific genes have been identified in both lymphatic and blood vascular endothelial cells in cultures.[23] Therefore, mAb availability would contribute to immunohistochemical identification of lymphatic vessels particularly in mice and understand the molecular basis of their functions. In the last two decades, several useful markers for lymphatic vessels have been reported. For example,
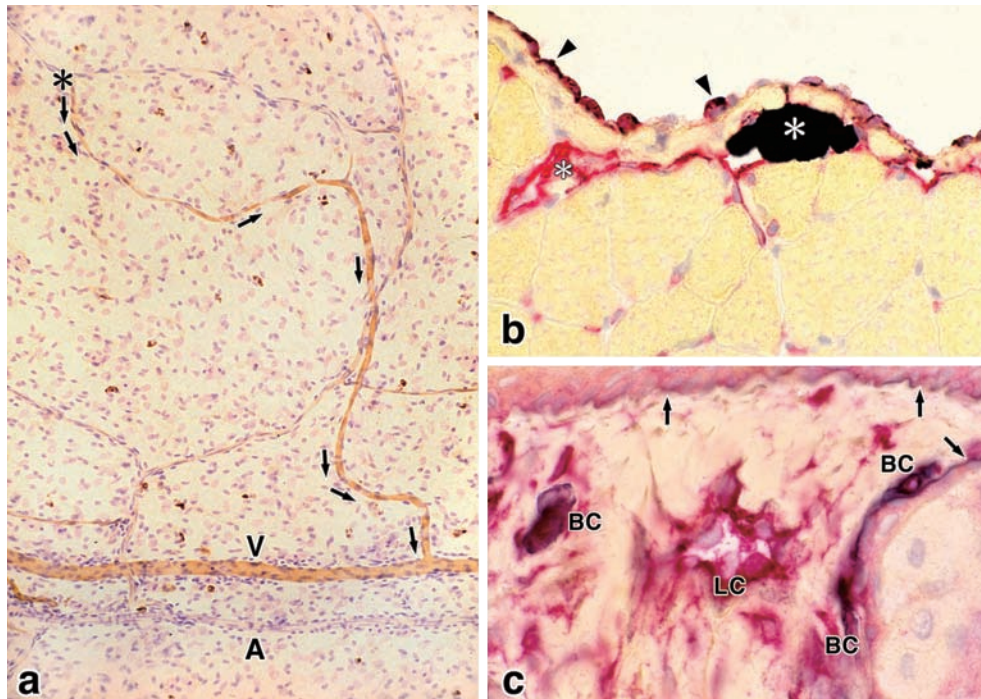
Figure 2 Specificity of B110 and B27 monoclonal antibodies to rat microvasculature.
a: Reactivity of B110 to capillary networks continuing two accompanying arteriole (A) and venule (V) in the mesentery. Note that B110 recognizes capillaries on the venous side (*starting point and flow direction: arrows) and venule (V), but not any arterial-type vessels including arteriole (A) as shown in Figure 1.
**b:** B27 recognizes lymphatic endothelial cells (red) of the lymphatic sinuses (＊: black carbon ink has been absorbed by the lymphatic vessels after a peritoneal injection) underlying the peritoneal surface of the diaphragm. Note that peritoneal mesothelial cells are also recognized by B27 and took up some carbon particles (arrowheads), suggesting their close relationship. (from Ezaki et al., 1990)[18]
c: As B27 also recognizes the endothelium of some types of blood vessels, it is necessary to combine double immunostaining of B27 (red) with type IV collagen of the basement membrane (arrows) to discriminate lymphatic capillaries and blood capillaries in sections of subcutaneous tissue of the skin. Note that lymphatic capillary (LC) is strongly stained by B27 (red), whereas blood capillaries (BC) are lined with basement membranes (dark brown). (from Ezaki et al., 1990)[18]

LYVE-1 is a specific receptor of hyaluronic acid.[24] Podoplanin is a marker for renal podocytes and is co-localized on lymphatic vessels.[25,26] Prox-1 is another nuclear marker for developing lymphatic endothelial cells.[27] However, most of these markers reported have not been originally discovered on lymphatic vessels; their empirical relationship with lymphatic vessels was realized accidentally.[20,24,25,27] Furthermore, their immunohistochemical distribution is not strictly confined to lymphatic endothelial cells, but shared with some blood vessel types.[20,28-30]

To discover novel lineage-specific markers of lymphatic origin, we sought to produce another mAb directed at mouse lymphatic endothelium.

However, there were several technical limitations. Firstly, the source material of lymphatics as an antigen for immunization is difficult to obtain. Secondly, lymphatic-specific antigens seem to have weak immunogenicity compared with those of blood vessels, against which several specific antibodies have been raised, probably due to their relatively strong immunogenicity. Lastly, there are no good screening procedures for selecting lymphatic-specific antibodies. To overcome these limitations, we applied several technical devices to obtain more confined lymphatic vessel-specific antibodies. We induced benign lymphangiomas in mice by intraperitoneal injection of Freund's incomplete adjuvant (FIA).[31]
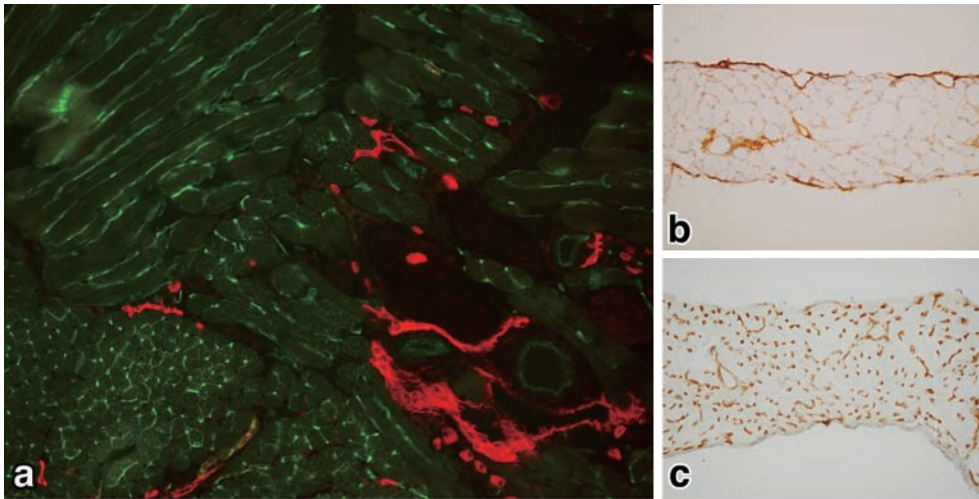
Figure 3 Reactivity of LA102 and LA5 to mouse vascular endothelial cells.
a: Double immunofluorescent staining of a C57BL/6 mouse tongue tissue section with LA102 (red) and LA5 (green). The distribution of both lymphatic and blood vessels in the tongue muscle layers is apparent.
b: Immunoperoxydase staining (DAB reaction: brown) of lymphatic vessels in the diaphragm are strongly stained with LA102.
c: Immunoperoxydase staining (DAB reaction: brown) of blood vessels in the diaphragm are stained with LA5.

This tumor model provided considerable amount of relatively pure source material of lymphatic endothelium.[32] Furthermore, we employed a mild enzyme treatment followed by the neuraminidase treatment[33] to expose very minor hidden cell surface antigens in lymphatic endothelial cells, and used a rapid differential immunization protocol to overcome the possible weak immunogenicity of lymphatic endothelial cells.[34] By trial and error, we successfully produced a rat mAb, LA102 (or LEC 26), reacting predominantly with mouse lymphatics, but not with any types of blood vessel. During the immunization, we could also obtain another mAb, LA5 (or BEC12), reacting selectively with most of peripheral blood vessels, but not to any type of lymphatic vessel (**Figure 3**).

These novel antibodies would prove useful for studies on mouse blood vascular and lymphatic microcirculation with several advantages.[34] First, the mAbs against vascular endothelial cells can be used to characterize and assess the functional properties of the antigens recognized. Second, confocal laser-scanning microscopy can be used for 3D imaging of the microvascular networks by infusing various fluorescent lectins into circulation (described later).

Third, endothelial cell proliferation can be identified by BrdU immunostaining of the tissue.[35] Finally, the functional aspects of microvessels can be further investigated by establishing some lymphatic endothelial cell lines in vitro after separating lymphatic endothelial cells from adjuvant-induced lymphangiomas. Several mouse lymphatic endothelial cell lines have been successfully established using these mAbs for positive separation using magnetic-activated cell sorting (MACS) (**Figure 4**). These cell lines can be useful to characterize lymphatic endothelial cells in vitro at the molecular level.[36]

3. Mouse Thy-1 antigen as a specific marker for lymphatic vessels

Interestingly, the antigen recognized by LA102 exists on not only lymphatic endothelial cells, but also some types of lymphoid cells, particularly the T-cell lineage cells. While characterizing the antigens recognized by this antibody, we found it to be a homolog of CD90.2 (Thy-1.2), but not CD90.1 (Thy-1.1). The following evidence supports this finding.

First, 94% of thymocytes and 51.2% of spleen cells were positive for LA102. The LA102-positive spleen cells were almost all positive for CD3. Second, T lymphocyte lineage-derived tumor cells were LA
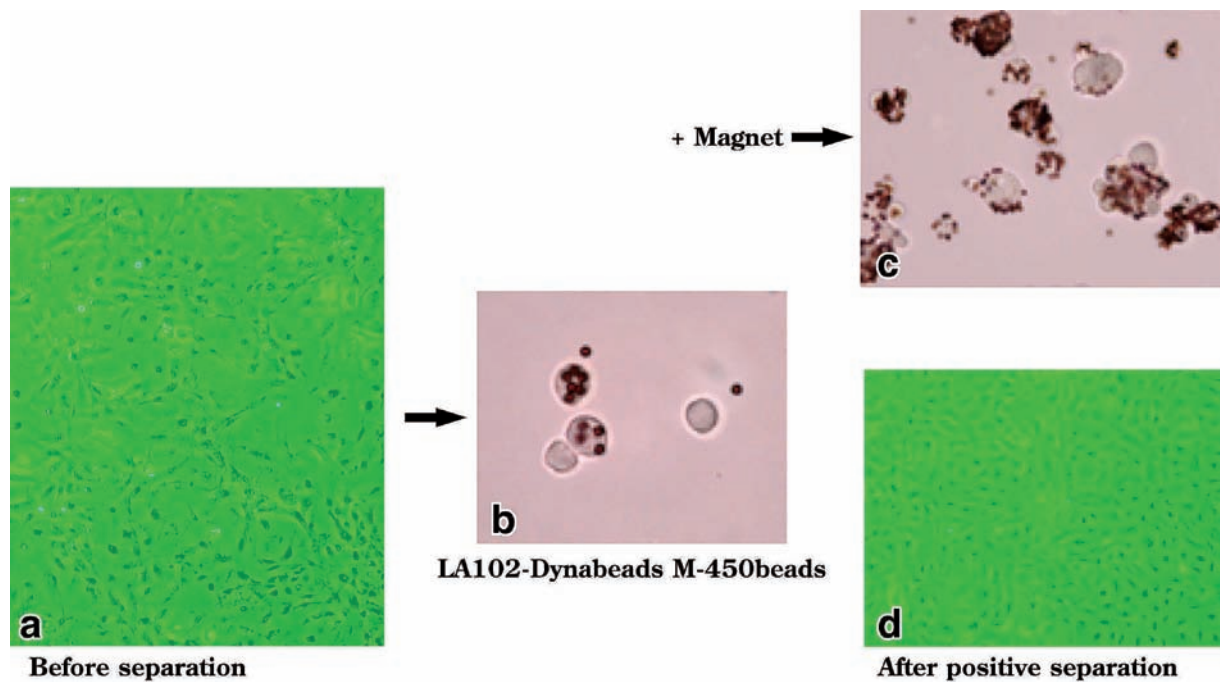
Figure 4 Positive separation of lymphatic endothelial cells from adjuvant-induced lymph-angiomas by MACS using magnetic beads conjugated with LA102.
a: FIA-induced lymphangiomas of C57BL/6 mice were digested with collagenase D (Boer-hinger-Mannheim Biochemicals: 2 mg/mL in RPMI1640 medium with 1% fetal calf serum) for 30 min at 37℃ and single cell suspension was prepared. The cell mixture was cultivat-ed as the primary culture for several days to obtain single cell layers. Note that the shape of cell mixtures varies, indicating that they are heterogeneous cell populations before positive separation. **b:** The cells were treated with 0.05% trypsin, collagenase (200 U/mL), and 1 mM EDTA in PBS at 37℃ for 30 min to obtain as single-cell suspension. The cells were then incubated with LA102-conjugated Dynabeads M-450 at 4℃ for 30 min. **c:** The cell mixture was then positively separated for LA102-positive cells by MACS. Note that all separated cells bear magnetic beads. **d:** After positive separation, the cells appeared almost homogeneous and like a cobble stone in cultures.

102 positive, but those from B lymphocyte and fi-broblast lineages were negative.[34] Third, LA102 only recognized its antigens on tissues from C57 BL/6, BALB/c, and DBA/2 mice (all Thy-1.2 back-ground), but not from AKR mice (Thy-1.1 back-ground) (**Figure 5a&b**). Forth, pre-treatment of tis-sue sections with phosphatidylinositol-specific phos-pholipase C from *Bacillus cereus* (PI-PLC) (P 5542-5 UN; Sigma-Aldrich, St. Louis, MO, USA) substan-tially diminished the reactivity of LA102 and Thy-1 antibodies against their original targets (**Fig-ure 5c-e**). This indicates that the antigen molecule recognized by LA102 is a glycoprotein anchored to the plasma membrane through a glycosylphosphati-dylinositol (GPI) tail covalently linked to the carboxyl-terminal amino acid. The GPI-anchored glycoproteins can be specifically cleaved off the cell membrane by phospholipase C treatment.[37] Finally, the molecular size of LA102 is approximately 26-27 kDa, which is almost equivalent to that of CD90, with 25-29 kDa in its reduced form. We also found that Thy-1.2 (CD90.2) is a homolog of LA102 in terms of molecular size and 45% mass-matching ra-tio in a mass-spectrogram analysis between the two molecules as well as their tissue co-localization (un-published data). These data suggest that Thy-1 (CD 90) is another specific marker for lymphatic endo-thelial cells in mice. Jurisic et al.[38] also reported that mouse lymphatic endothelial cells express high lev-els of Thy-1 in situ and in vitro.

Thy-1 glycoprotein has been well characterized in rodents and other species[39] since it was first de-scribed in 1964.[40] Thy-1, the smallest member of the immunoglobulin superfamily, is classified as a CD90
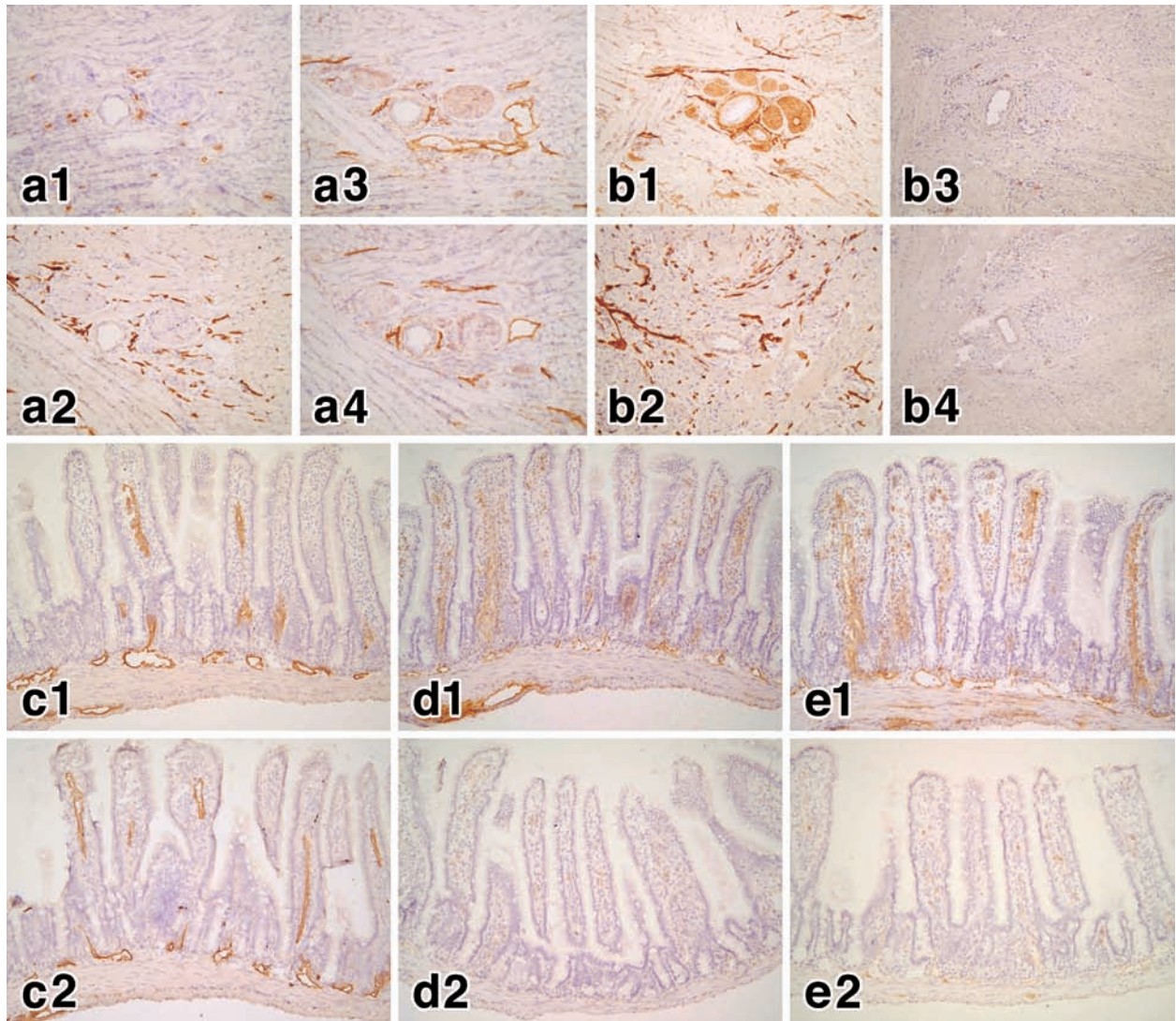
Figure 5 Effects of Thy-1 background and phospholipase C treatment on the antigens recognized by LA102 and other antibodies.

a: Cryosections of the tongue of C57BL/6 mice (Thy-1.2 type background) were stained by the immunoperoxidase reaction (DAB: brown) with either an anti-Thy1.1 antibody (a1), LYVE-1 (a2), an anti-Thy1.2 antibody (a3), or LA102 (a4). Note that no lymphatic vessel structure is recognized by the anti-Thy1.1 antibody, whereas the lymphatic vessels in the tongue are strongly stained by other antibodies including LA102. The positive stains in a1 are non-specific background stains (mainly of plasma cells, but not lymphatic vessels).

b: Cryosections of the tongue of AKR mice (Thy-1.1 type background) were stained by the immunoperoxidase reaction (DAB: brown) with either an anti-Thy1.1 antibody (b1), LYVE-1 (b2), an anti-Thy1.2 antibody (b3), or LA102 (b4). Note that no lymphatic vessel structure is recognized by both the anti-Thy1.2 antibody and LA102, whereas the lymphatic vessels in the tongue are strongly stained by the anti-Thy1.1 antibody and LYVE-1. The positive stains in b3 and b4 are non-specific background stains, but not any lymphatic vessel structures.

c-e: Cryosections of the tongue of C57BL/6 mice (Thy-1.2 type background) were treated either without (c1, d1, e1) or with (c2, d2, e2) phospholipase C (0.2 U/mL: Sigma) in 10 mM Tris buffer with 0.05% BSA for 30 min at 37℃ , and then stained by the immunoperoxidase reaction (DAB: brown) with LYVE-1 (c1, c2), LA102 (d1, d2), or an anti-Thy1.2 antibody (e1, e2). Note that phospholipase C treatment completely diminished immunostaining of both LA102 (d2) and anti-Thy1.2 antibody (e2), but not that of LYVE-1 (c2), indicating that the antigens recognized by LA102 and anti-Thy1.2 antibody are both GPI-anchored glycoproteins.

of size 25-29 kDa in its reduced form. Surprisingly, CD90 is differentially expressed and distributed among species and tissues of the same species. In human, CD90 is widely expressed on the surface of neuronal and various stromal cells, but only on a few blood leukocytes or lymphocytes.[41] In rodent, CD90 is present on various cells including thymocytes, peripheral T lymphocytes, nerve cells, fibroblasts, myoblasts, epidermal cells, and bone marrow stem cells.[42] As CD90 is highly expressed on rodent thymocytes, it is regarded as a differentiation marker for mouse T lymphocytes.[43,44] Moreover, in human and rat, CD90 is a marker for blood vessel endothelial cells and fibroblasts.[45-47] Indeed the diverse distribution of CD90 indicates that it plays some significant roles in different tissues and species.[48] However, its exact functions and natural ligands are still unknown. Because it belongs to the Ig superfamily, it is suggested that it has acts as a cell adhesion molecule and mediates some cell-to-cell interactions. CD90 has been reported to play potential role in cell adhesion required for tumor progression and inflammation.[38]

The most obvious difficulty in assigning a single function to the molecule is its unusual distribution.[39] It is not only present on various cell types in a species, but also on different cell types in different species. In mice, amino acid polymorphism exists in thymocytes and brain Thy-1 with two allelic forms-Thy-1.1 (CD90.1) and Thy-1.2 (CD90.2)—defined using alloantisera.[49] The only difference in amino acid in the extra membranous portions of Thy-1.1 and Thy-1.2 in mouse brain is Arg and Gln that interchange at residue 89, respectively.[50] As LA102 is a homolog of Thy-1.2, further investigation on their molecular characteristics is required.

4. Application to 3D-imaging of lymphatic vessels by various imaging techniques

1）Basic research using various imaging strategies

Although various novel lymphatic endothelial cell (LEC) markers have been discovered and information on lymphatic system has been accumulated, the distribution of each marker antigen does not necessarily coincide with each other. Therefore, it is difficult to differentiate LECs from other cell lineages, such as blood endothelial cells (BECs) and lymphoid cells. Specific marker availability for LECs enables the characterization of lymphatic function and visualization of lymphatic vessels at the 3D level.[51] Herein, I will focus on the diversity of LEC markers by immunohistochemical characterization of antigen distribution with mAbs and other useful markers. In studies on angiogenesis or vasculogenesis, the special relationship between newly formed vessels and existing vessels should be analyzed by 3D-imaging. This is because there is a limitation to understanding the actual 3D distribution of vascular networks on usual tissue sections (**Figure 6a&b**). By the mid 1990s, several sophisticated techniques have been developed and applied for 3D-imaging of microvasculature, such as vascular casts observed by the scanning electron microscopy (SEM) (**Figure 6c**). In addition to specific mAbs, various lectins[52] that recognize specific sugar chain residues can also be used to identify specific parts of BECs (**Figure 6d**). We have also successfully applied various lectins to identify tissue-specific vascular endothelial cells in mouse[53] or placental villous cells in human.[54] Morikawa sought to define specific lectins that individually bound to vascular endothelial cells and LECs in mice.[55] The results revealed that ConA and MAL-I bound strongly to LECs than to BECs and mesothelial cells. In contrast, LEL bound to BECs and mesothelial cells, but not to LECs (**Table 1**). Although the binding of these lectins to endothelial cells is not strictly specific, the use of lectins is very useful, because these labeled lectins can be simply injected either intravenously or subcutaneously/intraperitoneally to vitally stained blood vessels or lymphatic vessels, respectively (**Figure 7**).

Furthermore, Isogai and his colleagues developed the live imaging technique[56] and studied lymphangiogenesis in zebrafish.[57] Using two-photon time-lapse imaging, they demonstrated that the thoracic duct endothelial cells are derived from primitive veins[56] and provided insights into the origin of lymphatic endothelial cells; they suggested that the mechanisms controlling endothelial cell differentiation differed in the head and trunk of zebrafish.[57] There-
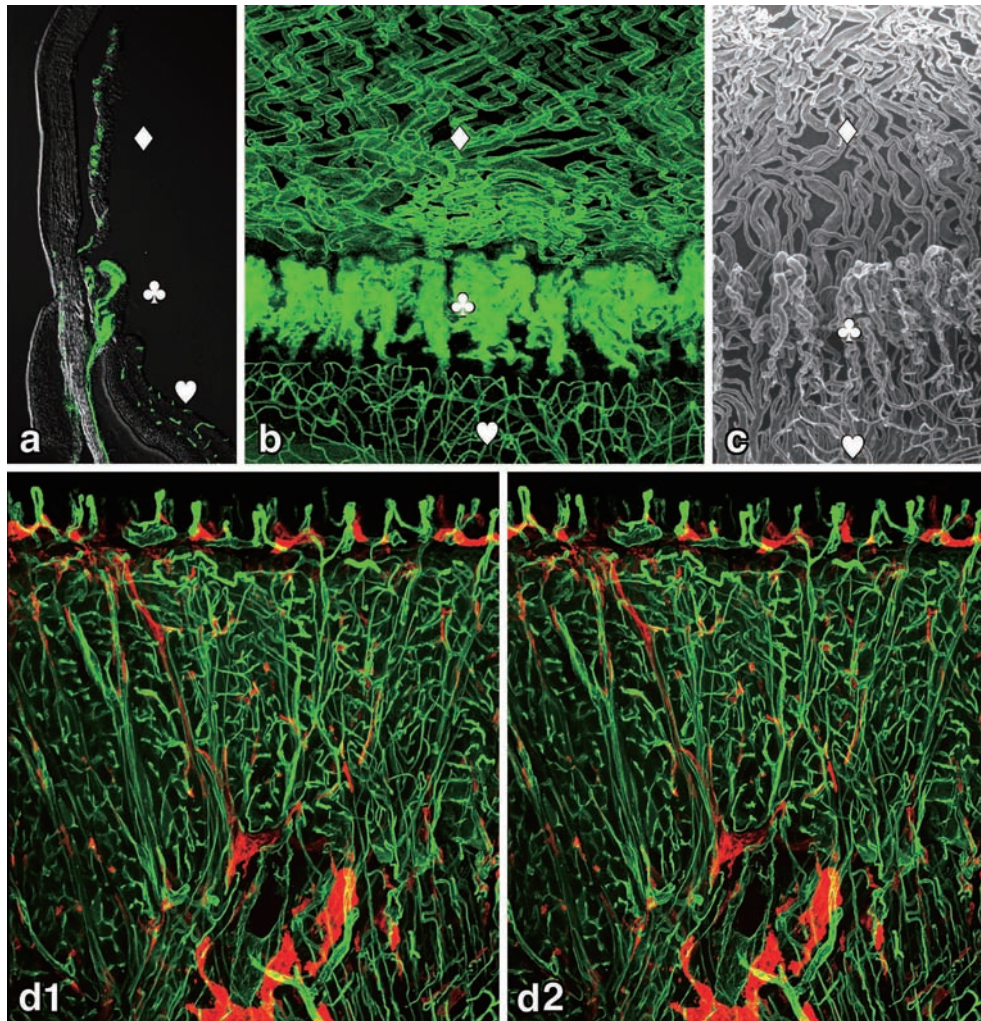
Figure 6 3D-imaging of uveal vascular structures and a stereoview of microvasculature in the mouse tongue using lectin.

a: A sagittal section of a mouse eye ball. Blood vessels were stained by intravenous injection of FITC-conjugated tomato LEL lectin (Vector Laboratories, USA) to label all the blood vessels (green). **b:** A whole-mount preparation of the anterior pole of a mouse eyeball. Blood vessels were stained in the same way as 6a. Note that the 3D-images of the vascular distribution patterns are completely different in each part of the uvea. **c:** The same view of the uvea of vascular corrosion casts by the scanning electron microscopy (SEM). Courtesy Prof. K. Toida (Kawasaki Medical School, Kurashiki, Japan). Blood vessels in the iris (◇), ciliary body (♧), and retina (♡) in a-c.

d: Stereo-pair immunofluorescent micrographs of a mouse tongue stained with FITC-conjugated tomato LEL lectin (Vector Laboratories, USA) (green) for blood vessels and LYVE-1 (red) for lymphatic vessels. The stereo-pairs of pictures, ±6° tilted (d1 and d2), were captured with the same magnification using a Leica TCL-SL confocal laser scanning microscope (Leica, Wetzlar, Germany). Capillary loops in the papillae and underlying lymphatics are clearly demonstrated.

fore, the spatial relationship between newly formed and existing vessels can be easily analyzed by 3D-imaging in studies on angiogenesis during various pathological conditions or vasculogenesis during development.

2) Clinical diagnostic and therapeutic applications

Lymphangiography has been used for clinical diagnosis when lipiodol or indigo carmine are subcutaneously injected, or ^{99m}Tc-labeled human albumin is applied for scintigraphy of lymphatics. However,

Table 1 Reactivity of various lectins to endothelial cells and mesothelial cells*.

Lectins	Sugar binding to	Lymphatic ECs	Blood vessels ECs	Mesothelial cells	Remarks
ConA	Mannose	++	+ (venules)	+	strong binding at stomata
LEL	GlcNAc	−	++	++	
MAL-II	Sialic acid	NT	NT	NT	
UEA-I	Fucose	−	−	−	
MAL-I		++	−	+	strong binding at stomata
RCA-I	Galactose /GalNAc	−	++	+	strong binding at stomata
GSL-I B4		++	++	+	blood vessel ECs stained with lectin i.p.

*Tested by S. Morikawa (unpublished data). All lectins were purchased from Vector Laboratories, USA.

EC, endothelial cell; i.p., intraperitoneal injection; NT, not tested.
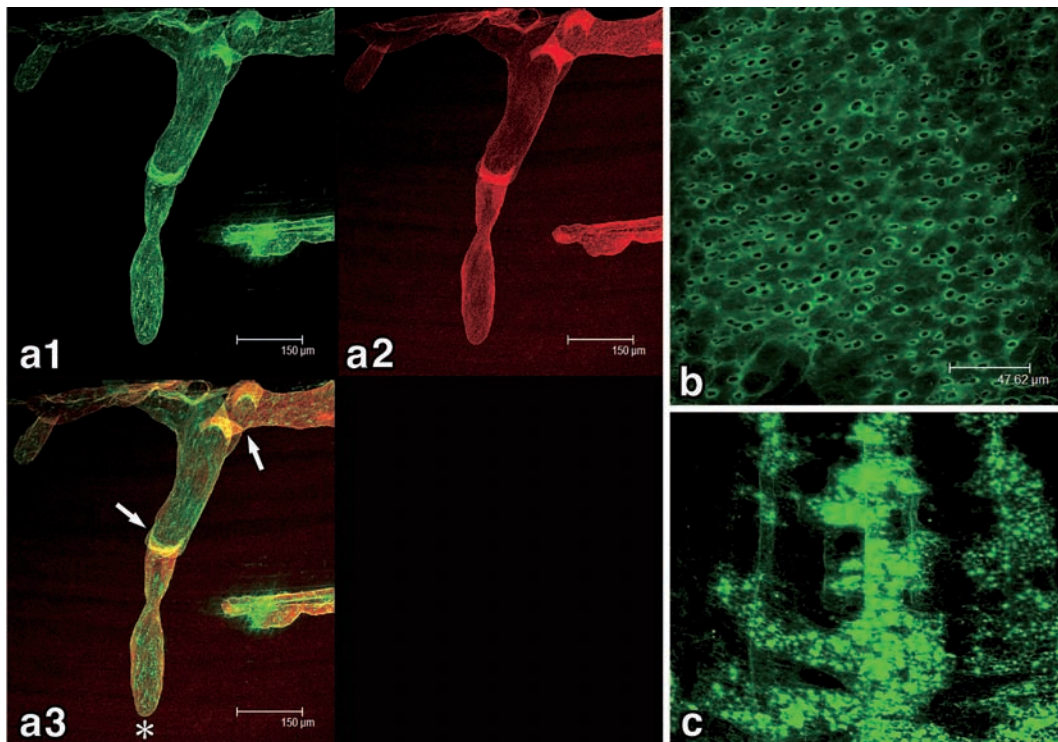
Figure 7 Identification of lymphatic vessels by lectins.
a: Confocal double fluorescent images of a lymphatic capillary (＊) in the thoracic side of the mouse diaphragm stained by intraperitoneal injections with FITC-conjugated MAL-1 (Vector Laboratories, USA) (a1: green) and LA102 (a2: red). The merged image (a3). The blind end (＊) of the lymphatic capillary and subsequent collecting vessel portion with valves (arrows) are clearly seen.
b&c: Confocal fluorescent images of the macula cribriformis on the peritoneal surface of the mouse diaphragm (b) and lymphatic sinuses (c) immediately underneath the mesothelium of the diaphragm stained by the intraperitoneal injection of FITC-conjugated ConA (Vector Laboratories, USA) (green).

side effects of such tracer substances are a concern. In addition to the radioactive substances, lipiodol of iodine compounds derived from lipid-soluble contrast media might cause embolization or allergic reactions to iodine. Pigmented solutions such as indigo carmine or isosulfan blue remain for a long period in the subcutis. Therefore, lymphangiography using new fluorescent dyes, such as indocyanine green (ICG), and magnetic resonance imaging (MRI) are more often applied for lymphatic vessel imag-

ing. Indocyanine green was first introduced in fluorescent lymphangiography to assess lymphatic function in patients with edema.[58] Since the proposal of the sentinel node theory by Morton et al.,[59] ICG has become one of the most commonly used tracers in clinical diagnosis and navigation surgery for malignant diseases.[60,61] Advanced MRI for lymphatic vessels[62] and real-time imaging of the lymphatic system using ultrasonography and Sonazoid[63] are also reported to visualize various lymphatic vessels.

Unveiling the Relationship Between Peritoneal Mesothelium and Lymphatic Endothelium

The lymphatic system plays important roles in draining of tissue fluid and transport of lipids, macromolecules and immune cells. The actual mechanisms underlying its key function, such as the selective uptake of materials, are yet to be established. Both fluid drainage and cell trafficking in the body cavity, particularly peritoneal cavity, are clinically important for the pathogenesis of ascites, inflammation, and malignant cell metastasis. There are several studies on lymph drainage from the peritoneal cavity.[64-68] The rate and pattern of absorption of liquid, cells, and insoluble particulates differ with materials. Fritz and Waag[69] have reported the transdiaphragmatic lymphatic transport of intraperitoneally administered particulate marker. Bettendorf[70,71] reported the peritoneal resorption of latex particles via diaphragmatic lymphatics. However, his studies have mostly focused on the normal structural and functional aspects of routes of lymph absorption of various materials under physiological conditions. Yuan et al.[72] reported the lymphatic drainage of inflammatory cells from the peritoneal cavity in a sheep peritonitis model. The obstruction of lymph drainage or other lymphatic disorders under pathological conditions may also be important issues in clinical treatments for ascites.

In order to establish a tumor model for studies on the lymphatic drainage from the peritoneal cavity, we induced benign lymphangiomas in rats[32] and mice[73,74] by intraperitoneal FIA injection according to the method of Mancardi et al..[31] This tumor model could help unveil the relationship between peritoneal mesothelium and lymphatic endothelium.

1. General changes in the peritoneal cavity surface after FIA injection

We first performed morphological and functional characterization of FIA-induced lymphangiomas with respect to their phenotypes and effect on lymph drainage from the peritoneal cavity in rats.[32] In approximately two months after the intraperitoneal FIA injections (1 mL emulsion) with a two-week interval, tumors developed in the peritoneal cavity, such as the diaphragm, omentum, and liver surface. To distinguish lymphatics from blood vessels, various mouse mAbs against rat microvasculature (B27, B1, and B110) were used. We also used a tomato lectin (*Lycopersicon esculentum* lectin, LEL) for blood vessel staining[35] and 5'-nucleotidase reactivity[75] for lymphatic vessel staining. We found that the tumors themselves lacked the typical lymphatic phenotypes, but were partly positive for blood vessel markers (B1). Type IV collagen was negative or very weakly positive. The results suggest that these tumors might share some characteristics of both lymphatic capillaries (5'-nucleotidase: partly strong-positive) and arterial-side capillaries (B1: positive), although they showed a honey comb-like or granulomatous morphology.[76] However, the draining capacity of lymphangioma via diaphragmatic lymphatics to parathymic lymph nodes was remarkably reduced, indicating that the tumor lost its absorptive function as lymphatics.[32]

We then investigated the phenotype of the tumor in depth in mice.[73] Interestingly, within three days after a single intraperitoneal FIA injection, the peritoneal cavity surface started to change and formed typical benign lymphangiomas (**Figure 8a-d**). One to two weeks after FIA injection, we found that peritoneal mesothelial cells elongated (cuboidal) and lost their polarity, and gradually formed thick stratified cell masses all over the peritoneal membrane (**Figure 8c&d, 9a-e**). By day 3 of FIA injection, we found an increase in the early pregnant factor (EPF or HSP-10)[77] and podoplanin expression in peritoneal mesothelial cells (**Figure 8e&f**). EPF has been reported to be produced and secreted into blood by some types of mineral-oil-induced tumor.[77,78] In our
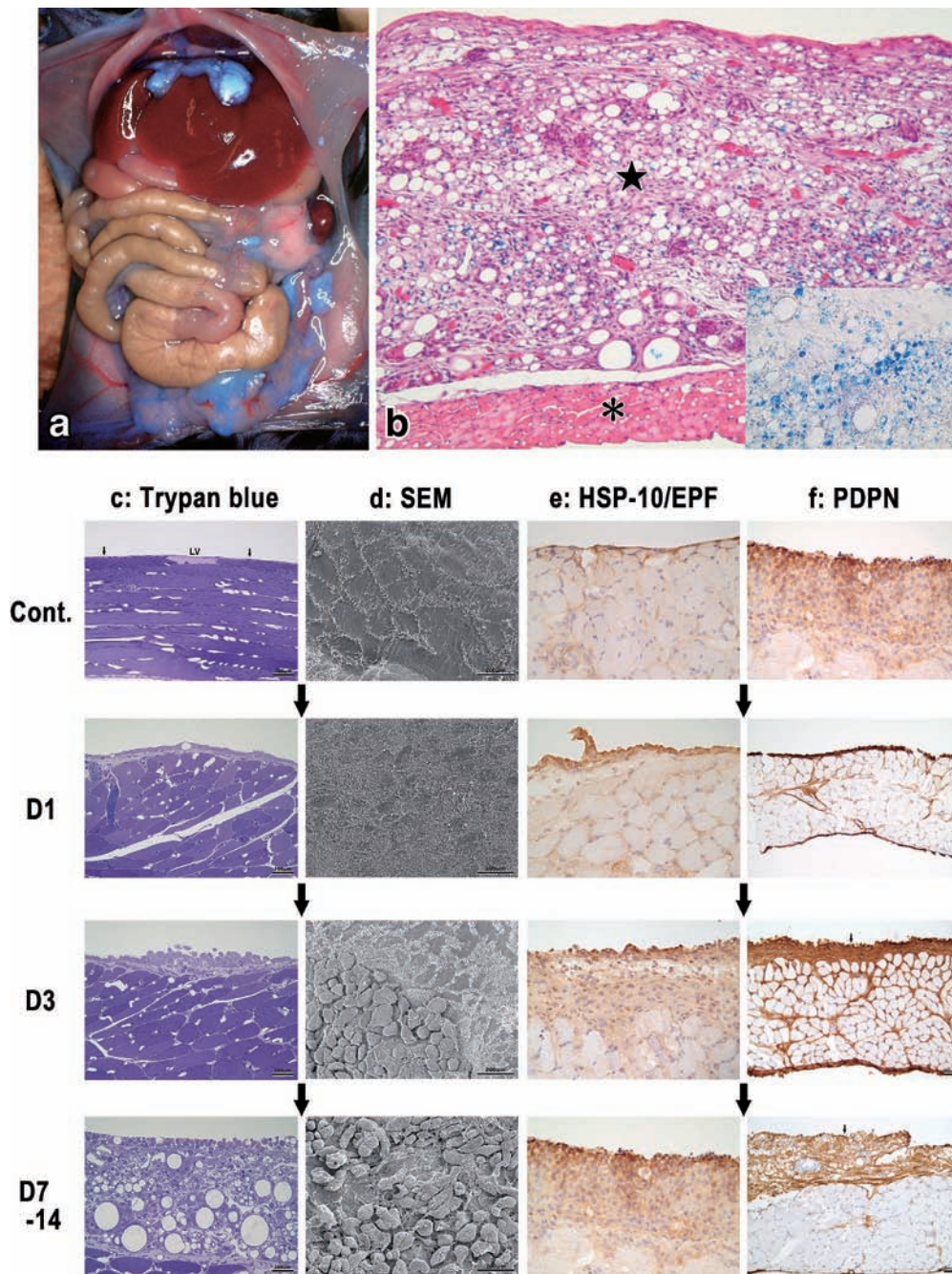
Figure 8 Development of lymphangiomas induced by a peritoneal FIA injection in mice.
a: A macroscopic view of peritoneal cavity in a mouse two weeks after a peritoneal FIA injection containing EM-blue (blue dye). Note that not only the surface of the liver, diaphragm, and mesenteries including the omentum, but also the surface of abdominal walls colored blue, indicating FIA is taken up by lymphangiomas developed almost all over the peritoneal surface. **b:** Light microscopic view of the lymphangioma (★) developed on the surface of the diaphragm (*) four weeks after the FIA injection (Hematoxylin and Eosin staining). Note that FIA containing EM-blue dye is taken up by the tumor cells (inset: a higher magnification of the tumor without HE staining). **c-f:** Sequential changes of the abdominal surface before (Cont.) and after FIA injection (D1: day 1, D3: day 3, D7-14: day 7-14). The tumor development were observed by semithin epon sections stained with trypan blue (c), scanning electron microscopy (d: SEM), cryosections stained by the immunoperoxidase reaction (DAB: brown) against mouse HSP-10/EPF (R&D Systems, Inc.) (e), and also against mouse podoplanin (AngioBio Co., USA) (f: PDPN). Note that not only peritoneal mesothelial cells but also many peritoneal free cells (some of them bearing large vacuoles) are seen on the surface of the lymphangiomas (in c&d: D3, D7-14).
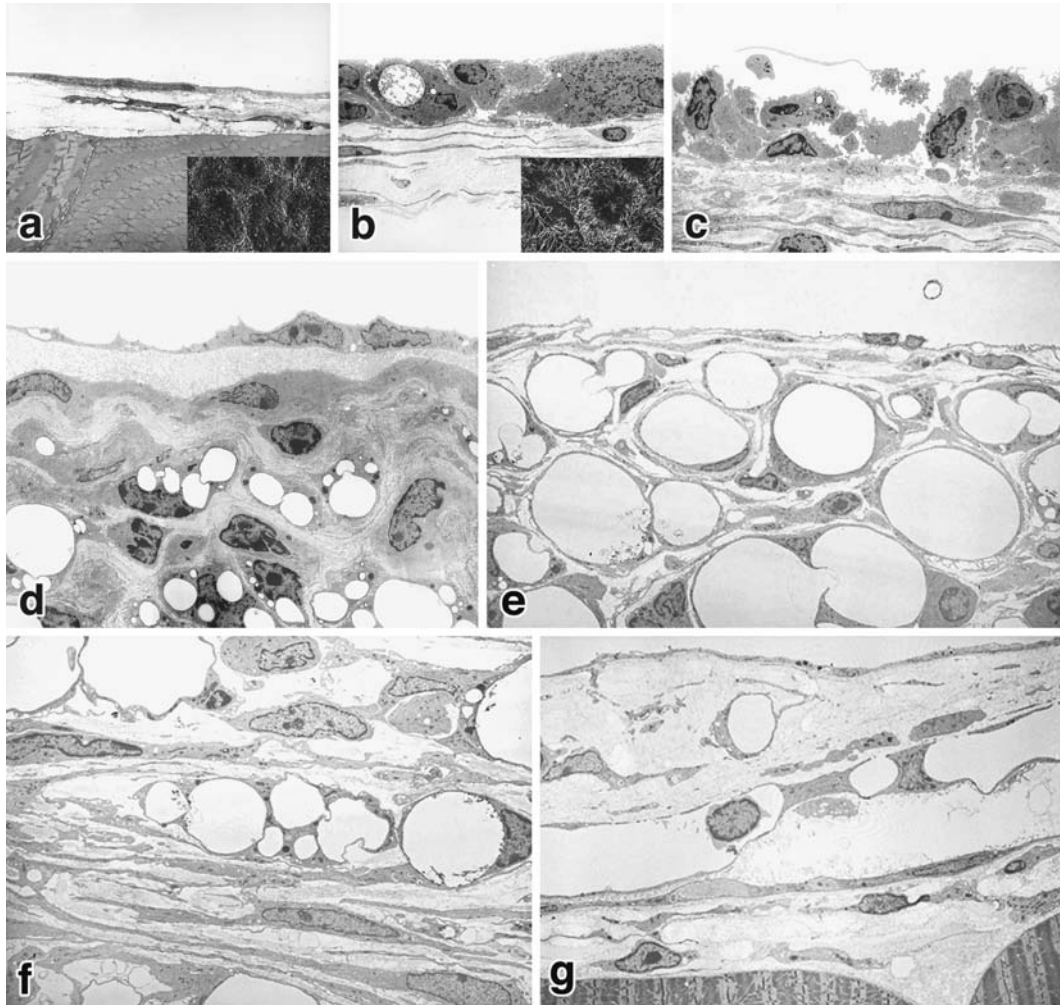
Figure 9 Ultramicroscopic changes of the lymphangiomas after FIA injection.
Transmission electron micrography (TEM) and scanning electron micrography (SEM) were performed to characterize the lymphangiomas at electron microscopic level. **a:** Normal surface of the peritoneal wall. The SEM image (inset) of the mesothelium. The mesothelial cells are simple squamous with short microvilli on their surface toward the peritoneal cavity. **b:** Three to five days after FIA injection. The SEM image (inset) of the mesothelium. Note that the mesothelial cells became taller and cuboidal, with increased microvilli all around the cell surface, indicating they have lost their polarity. Some cells take up FIA into their cytoplasm. **c-d:** One to two weeks after FIA injection. Mesothelial cells have loosened the cellular connections with each other, and then several peritoneal free cells attach and get further into the interstitial spaces underneath mesothelial cells (c). Some mesothelial cells formed multilayers with abundant and long microvilli on the bilateral sides of their surface. Several cells in the newly formed tumors have various sizes of fat (FIA) droplets (d). (from Ezaki and Desaki, 2012)[73] **e:** At four weeks or later, the fat droplets fused with each other and increase in size in the cells. The fat-storing cells became larger in size, and then some adjacent cells gradually fused with each other to form cell clusters. **f-g:** At two to four months or later, the fat-storing cells fused with each other and gradually formed tubular structures like lymphatic vessels. (from Ezaki and Desaki, 2012)[73]

model, EPF might have been induced locally **(Figure 8e)**, but its serum level was unaltered at least until seven days (unpublished data). Contrarily, the increase in local podoplanin expression was remarkable and the whole lymphangiomas became strongly positive **(Figure 8f)**. However, the tumor contained some LA5⁺ blood vessels, but not LYVE-1⁺ or LA102⁺ cells. This suggests that the tumor itself is mesothelial in origin, rather than lymphatic endothelial cells. By day 7-14, the tumors showed

heterogeneous expression of lymphatic endothelial markers. At four weeks or later, they formed typical honeycomb-like lymphangiomas consisting of various-sized fat-storing cells (**Figure 8b, 9d-f**). As they developed, the fat-storing cells fused with each other and gradually formed tubular structures like lymphatic vessels (**Figure 9e-g**) or large follicles. Consequently, LYVE-1^{+} and LA102^{+} functional lymphatic vessel structures were detected at approximately four weeks after FIA injection as described later. These sequential changes appear to be unique if the phenomenon is regarded as a process in lymphangiogenesis. Shimizu et al. also found similar vasculogenic patterns, where individual LYVE-1^{+} stromal cells gathering around the trabecular arteries gradually joined and fused together, and finally formed various tubular structures as the initial lymphatic in developing spleen at 18.5 days of the embryonic age in mice (unpublished data).

2. Morphological and functional phenotypes of cells involved in FIA-induced lymphangiomas

Although the tumors were podoplanin[+], typical lymphatic vessel-like structures expressing LYVE-1 and LA102 only appeared at the later stages (four weeks or later). Therefore, the initial name "lymphangioma" for this animal tumor model[31] might not be suitable. This idea prompted us to characterize the phenotype of the adjuvant-induced tumor.

To clarify the involvement of bone marrow-derived cells in tumor development, GFP[+] bone marrow cells (1.5×10^7 cells/100 μL) from C57BL/6 (GFP-Tg) mice were intravenously injected to lethally irradiated (12 Gy) syngeneic mice. The recipient bone marrow chimeric mice were intraperitoneally injected FIA (0.2 mL) two weeks after bone marrow cell transplantation. Substantial number of GFP^{+} cells accumulated in FIA-induced lymphangiomas from the beginning of tumor development (**Figure 10a&b, e-h**). We confirmed that most of these cells had some macrophage or myeloid cell markers, such as CD68 (**Figure 10c**), Gr-1 (**Figure 10d**), and CD11c (figure not shown). We also found that some interstitial cells bearing fibroblast marker (S100A4) were involved in this tumor (figure not shown). Therefore, we concluded that lym-

phangiomas of several cell origins including at least mesothelium, macrophages, and fibroblasts were formed as chimeric cell masses by fusing with each other to dispose the extrinsic FIA. In other mineral oil-induced tumors, besides granulomatous responses that might correspond to our tumor model, plasmacytomas were quite common.[76,79] Interestingly, there was a strain difference in the incidence of plasmacytomas, but there were no reports regarding this in oil-induced granulomas.[80] Furthermore, the involvement of M1 (iNos[+]) and M2 type macrophages (arginase[+]) was compared on days 3 and 120 after the FIA injection. (**Figure 10e-h**) On day 3, both M1 proinflammatory and M2 anti-inflammatory macrophages increased in the tumors, whereas only a few M2 type macrophages were found in the tumors at very late stage (day 120). However, further studies should be conducted to clarify the biological significance of M1/M2 macrophage balance[81,82] in this tumor model.

Gene expression levels of podoplanin, CCL2, Prox-1, TGF-β, VEGFc, and TNF-α in lymphangiomas were examined using RT-PCR at various times after FIA injection (**Figure 11**). Considerable increase in podoplanin and CCL2 expression was observed by day 1, and an increase in TGF-β and VEGFc from day 3. However, one of the lymphatic endothelial markers, Prox-1, did not show any significant change. A remarkable increase in podoplanin expression was also confirmed in tissue sections. As podoplanin^{+} cells secrete CCL2 to recruit CD68^{+} cells in wound-healing lesions,[83,84] the increase in podoplanin and CCL2 expression in lymphangiomas might support the massive accumulation of bone marrow-derived macrophages (CD68^{+} cells) from the peritoneal cavity into tumors.

Furthermore, we investigated the expression of various fat-storing-cell-related markers in lymphangiomas. For example, adipophilin is known to be positive for fat-accumulating hepatocytes in alcoholic cirrhotic fatty livers or lipid-storing CD68^{+} macrophages. Both adipophilin^{+} and CD36^{+} cells might correspond to CD68^{+} macrophages.[85,86] We found a considerable increase in cells positive for adipophilin and CD36 (**Figure 12a&b**). Fat-droplet-
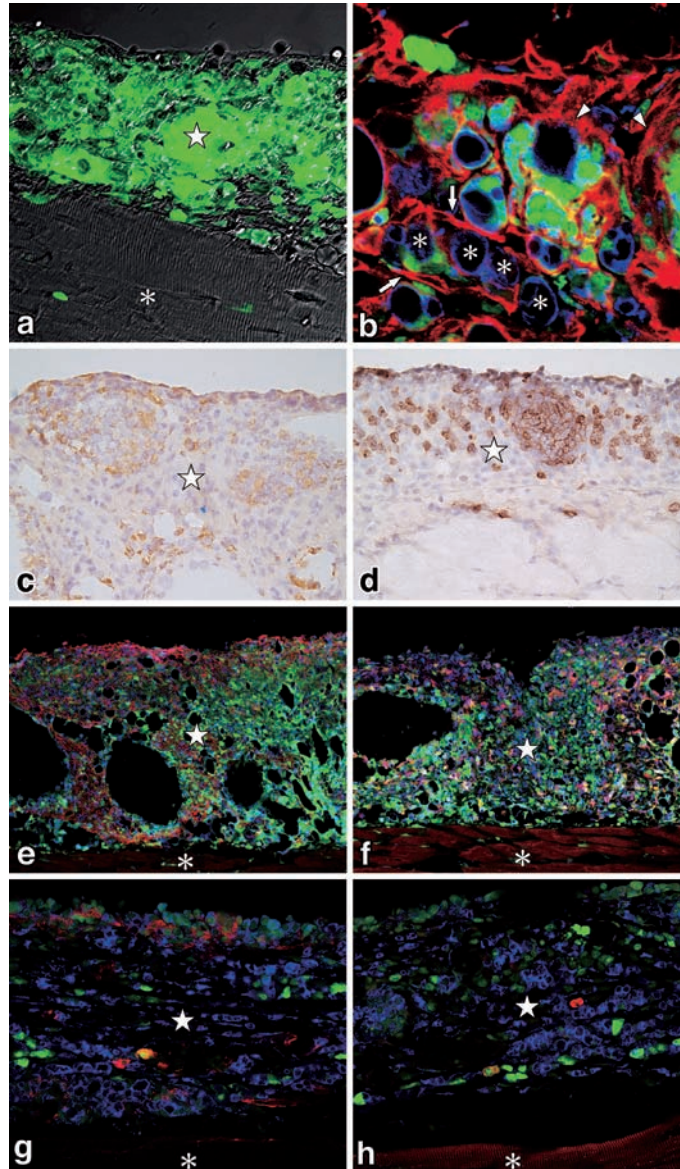
Figure 10 Involvement of bone marrow-derived intraperitoneal cells in FIA-induced lymphangiomas.

a: GFP+ (green) bone marrow-derived cells accumulated in lymphangiomas (☆) developed on the muscular layer of the diaphragm (✱) seven days after FIA-injection. **b:** Confocal triple immunofluorescent image of the cellular masses in lymphangiomas of GFP+ bone marrow cell-reconstituted mice four weeks after the FIA injection. GFP (green), podoplanin (red), and CD68 (blue). Note that the cell masses are found to be chimeric cell mixtures (arrowheads) from different origins and many of them contain various sizes of fat droplets (✱). Podoplanin+ cells (arrow) surround these cell mixtures. **c:** Immunoperoxidase staining of lymphangiomas developed two weeks after the FIA injection for CD68, a macrophage marker. **d:** Immunoperoxidase staining of lymphangiomas developed two weeks after the FIA injection for Gr-1, a myeloid differentiation antigen (Ly-6G/Ly-6C).

e-f: Confocal triple immunofluorescent image of the cellular masses in lymphangiomas of GFP+ bone marrow cell-reconstituted mice three days after FIA injection. Both M1 (red in e: iNos) and M2 (red in f: arginase) type macrophages (CD68: blue) were located in lymphangiomas at a very early stage of tumor development. **g-h:** Confocal triple immunofluorescent image of the cellular masses in lymphangiomas of GFP+ bone marrow cell-reconstituted mice 120 days after the FIA injection. Note that there are some M1 type macrophages (red in g: iNos) are still present in lymphangiomas, but a very few M2 type macrophages (red in h: arginase). ☆: lymphangioma, ✱: muscular layer of the diaphragm in c-h.
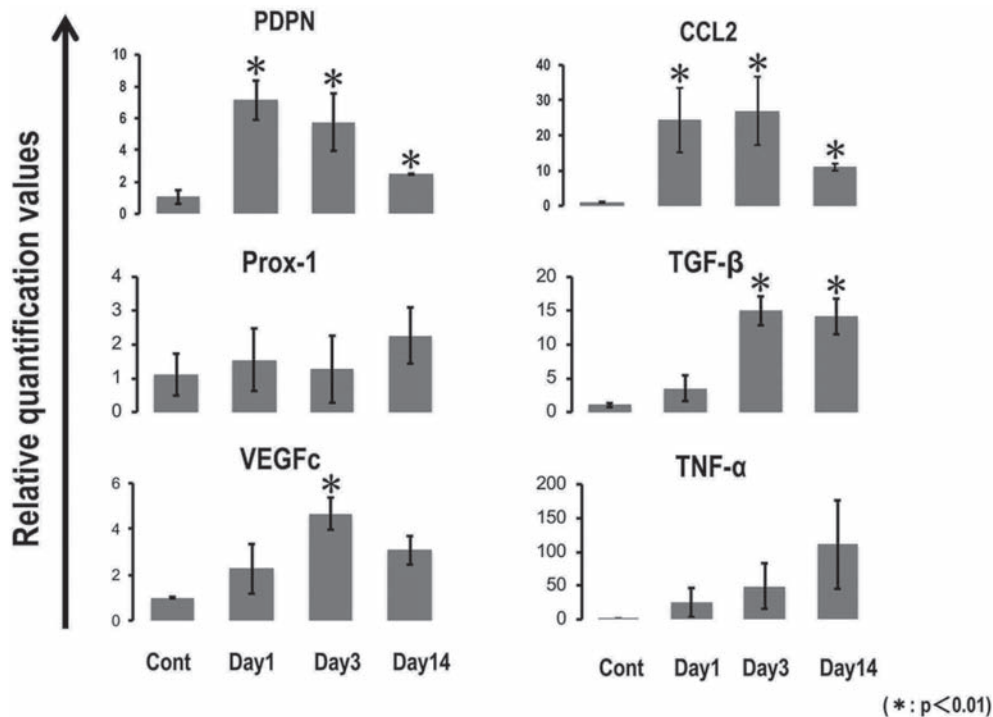
Figure 11 Expression level of lymphatic and inflammation related factors in the diaphragm using the RT-PCR assay.
A quantitative analysis was performed using the RT-PCR to determine the expression level of podoplanin (PDPN), CCL2, Prox-1, TGF-β, VEGFc, and TNF-α in the diaphragm at various times (control, and days 1, 3, and 14) after FIA injection. The results were normalized using β-actin as the internal control. To calculate the expression level of genes, the delta-delta comparative threshold method was used. Note that remarkable increases in PDPN and CCL2 expression were seen as early as day 1, and an increase in TGF-β and VEGFc from day 3. However, one of the lymphatic endothelial markers, Prox-1, did not show any significant change (*p < 0.01). (from Ezaki et al., 2018)[74]

storing cell accumulation in tumor might be similar to the pathogenesis of atherosclerotic plaques in the arterial wall where lipid droplet-containing macrophages also accumulate.[87,88] Interestingly, both these phenomena are closely related to lipid or oil that triggers macrophage infiltration under the endothelium or mesothelium in atherosclerosis or FIA-induced lymphangiomas, respectively. However, adiponectin **(Figure 12c)**, one of the major adipokines, production was not very significant.

The massive uptake of fat (FIA) into lymphangiomas prompted us to investigate fat metabolism in relation to fat droplets in the tumor. Fatty acid-binding proteins (FABPs) are known to be involved in promoting cellular uptake, and transporting and targeting fatty acids to specific metabolic pathways.[89,90] Therefore, we investigated the possible involvement of FABPs in FIA-induced tumor development using FABP-KO mice and specific antibodies against mouse FABP1, FABP3, FABP4, FABP5, and FABP7.[91] In normal C57BL/6 mice, a single peritoneal FIA injection induced typical honeycomb-like lymphangiomas consisting of various-sized ring-like fat-storing cells. These cells were strongly positive for podoplanin, F4/80, and FABP5 and FABP7. Contrarily, significant positive staining for FABP4 was not observed **(Figure 12d)**. In atherosclerosis, FABP4 (aP2 or adipocyte FABP) expression by macrophages promoted atherogenesis,[89] whereas FABP5 **(Figure 12e)**, rather than FABP4, appeared to be more responsible in our tumor model, and the follicular structures mainly consisted of FABP7^{+} cells **(Figure 12f)**. On the contrary, in FABP3-, FABP5-, FABP7-KO mice (data not shown), there was no significant difference in the incidence of tumors when compared with that
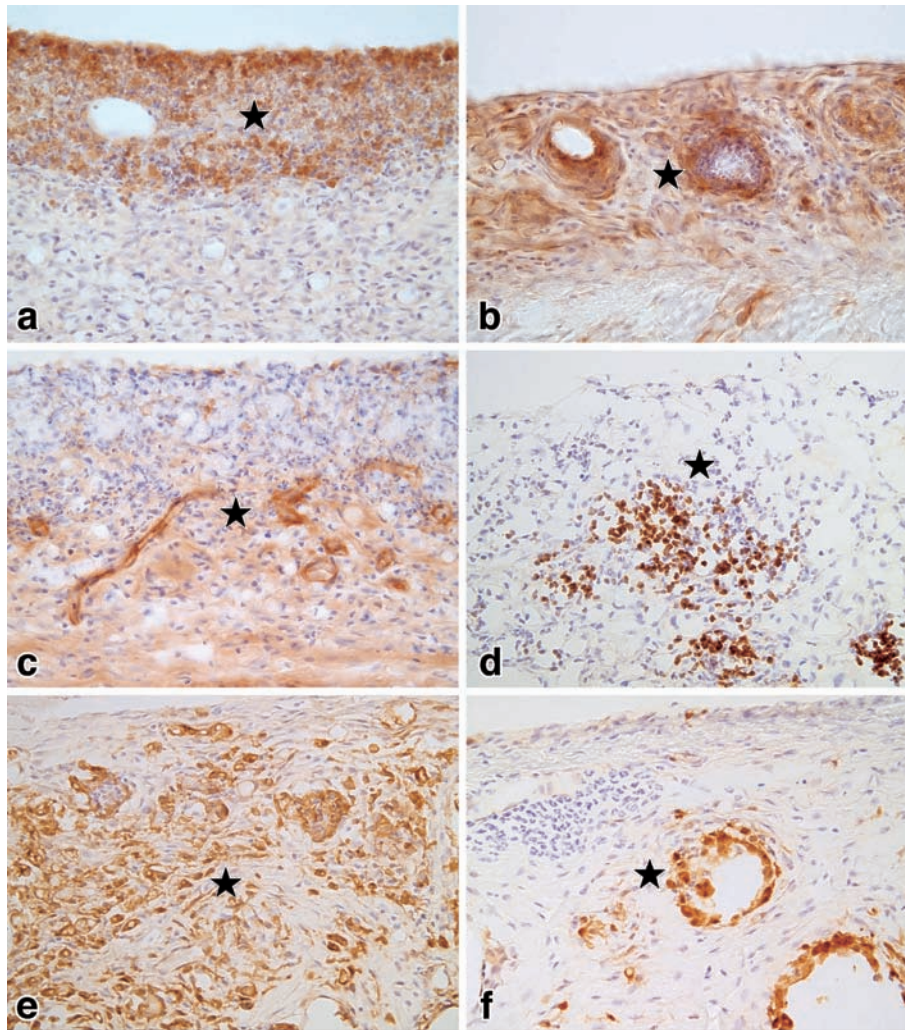
Figure 12 Expression of various fat-related markers in lymphangiomas.
a: Immunoperoxidase staining of lymphangiomas for adipophilin (PROGEN Biotechnik GmbH, Germany), a macrophage marker relating to lipid droplet-associated proteins.
b: Immunoperoxidase staining of lymphangiomas for CD36 (Cascade Bioscience, MS, USA), a macrophage marker also relating to lipid droplet-associated proteins. **c:** Immunoperoxidase staining of lymphangiomas for adiponectin (R&D Systems, Inc., USA), an adipokine.
d-f: Immunoperoxidase staining of lymphangiomas for FABP4 (d), FABP5 (e), and FABP7 (f). DAB^{+} cells in FABP4 staining (d) are non-specific background stains. All anti-FABP antibodies were gifted by Prof. Owada Y. (Tohoku University, Sendai, Japan). All cryosections of the lymphangiomas (★) developed two to four weeks after FIA injection were colored by DBA reaction in a-f.

in normal B6 mice. However, tumors developed more vigorously in FABP7-KO mice than in other KO strains. Among FABP-KO mice, relatively smaller fat-storing cells were seen in FABP3-KO mice, whereas the follicle-type structures were more commonly found in FABP5-KO mice. In contrast, the tumors in FABP7-KO mice showed less fat-storing cells with more inflammatory and fibrous components. The results suggest that a close relationship between the extrinsic FIA metabolism and fat-storing cell mass is involved in this tumor model, because the tumor cells contain FIA in their cytoplasm as various-sized lipid droplets.[74] However, the actual role and biological significance of each FABP in the tumorigenesis remain to be further clarified.

During tumor development, the tumor contained some LA5^{+} blood vessels, but not LYVE-1^{+} or LA102^{+} cells until about four weeks after FIA injection. This was confirmed by other vascular mark-

ers, such as blood vessels with CD31 **(Figure 13a)** and lymphatic vessels with Prox-1 and VEGFR-3 (figure not shown). Only the typical lymphatic vessel-like structures expressed LYVE-1 and LA 102 at the late stages (four weeks or later) **(Figure 13c-f)**. This corresponds to the time when the tubular structures are found after fusion of various cell masses **(Figure 9e&f)**. Furthermore, vasohibin-2 (VASH2), a tumor angiogenesis-promoting factor, was detected in the tumor **(Figure 13b)**. It was expressed preferentially in mononuclear cells derived from the bone marrow and promoted angiogenesis in the mouse.[92] It is also known that VASH-2 is required for epithelial-mesenchymal transition of ovarian cancer cells via regulation of TGF-β signaling.[93] As the tumors develop, the fate of extrinsic FIA might be a problem. In the tumor, we found abnormal draining routes from the peritoneal cavity at very late stages. Once the oil droplets are stored in cells, they are gradually secreted out of these cells into, for example, follicular structures **(Figure 14a&b)**, or through the remodeled lymphatic vessel-like structures **(Figure 9g, 13c&d)**. They finally reached either the draining lymph nodes of peritoneal cavity **(Figure 14e)** or abnormal collateral routes penetrating abdominal wall to dispose FIA to the skin subcutis **(Figure 14f&g)**. The significance of these complementary transformations might involve tissue remodeling after acute or chronic inflammation and lymphangiogenesis to drain undesirable fat droplets in the peritoneal cavity.

3．Relationship between peritoneal mesothelium and lymphatic endothelium

The actual mechanisms underlying tumorigenicity of this tumor model is unclear. In the 1960 s, there were several reports on the development of variety of tumors after the intraperitoneal injection of some mineral oils or adjuvants.[79,80] Furthermore, in 1985, Leak et al.[76] reported that peritoneal mesothelium developed granulomatous tumors in response to mineral oil or pristane. Quinn[78] reported that EPF (or HSP-10) is involved in the initiation and maintenance of various peritoneal responses to mineral oil. We also found some mesothelial and in-

terstitial cells including fat-stored cells expressed EPF. During the first one or two weeks, a remarkable increase in EPF expression was observed in the tumors **(Figure 8e)**. However, the biological role of EPF in tumor development after FIA injection remains unclear. As EPF is produced during various responses under both physiological and pathological conditions,[77] there might also be some other factors involved in this tumor model; this should be further investigated.

The fact that peritoneal mesothelial cells became tall in height (cuboidal) and lost their polarity, and gradually formed thick stratified cell masses all over the peritoneal membranes one to two weeks after FIA injection may suggest the potential of the mesothelial cells to transform into benign tumors forming cell masses with other type of cells **(Figure 10b, 14b)**. The increase in podoplanin and its gene expression in FIA-induced tumors **(Figure 8f&11)** might also be related to the potential diversity of mesothelial cells and possible transformation into lymphatic endothelial cells. As podoplanin correlates with ezrin redistribution to membrane projections and cytoskeleton and cell motility regulation,[94] podoplanin might play a role in inducing these sequential changes in tumor progression by linking mesothelial and lymphatic endothelial functions. Leak et al.[76] also found that an intraperitoneal injection of pristane, a mineral oil, induced squamous mesothelial cells to become cuboidal and lose their polarity. They reported that pristane induced fibrin networks, as in inflammation, involving extracellular matrices, such as fibronectin, resulting in huge granuloma-like structures attracting peritoneal free cells. Simultaneously, vigorous angiogenesis and lymphangiogenesis occurred, probably due to platelet activation upon engagement by podoplanin.[94,95]

These results indicate that FIA-induced tumors are heterogeneous cell population forming chimeric cellular masses resulting from mutual cell fusion after fat droplet uptake. In addition to podoplanin^{+} mesothelial cells, bone marrow-derived macrophages (CD68^{+}), and some interstitial mesenchymal cells are also involved in tumorigenicity in this tu-
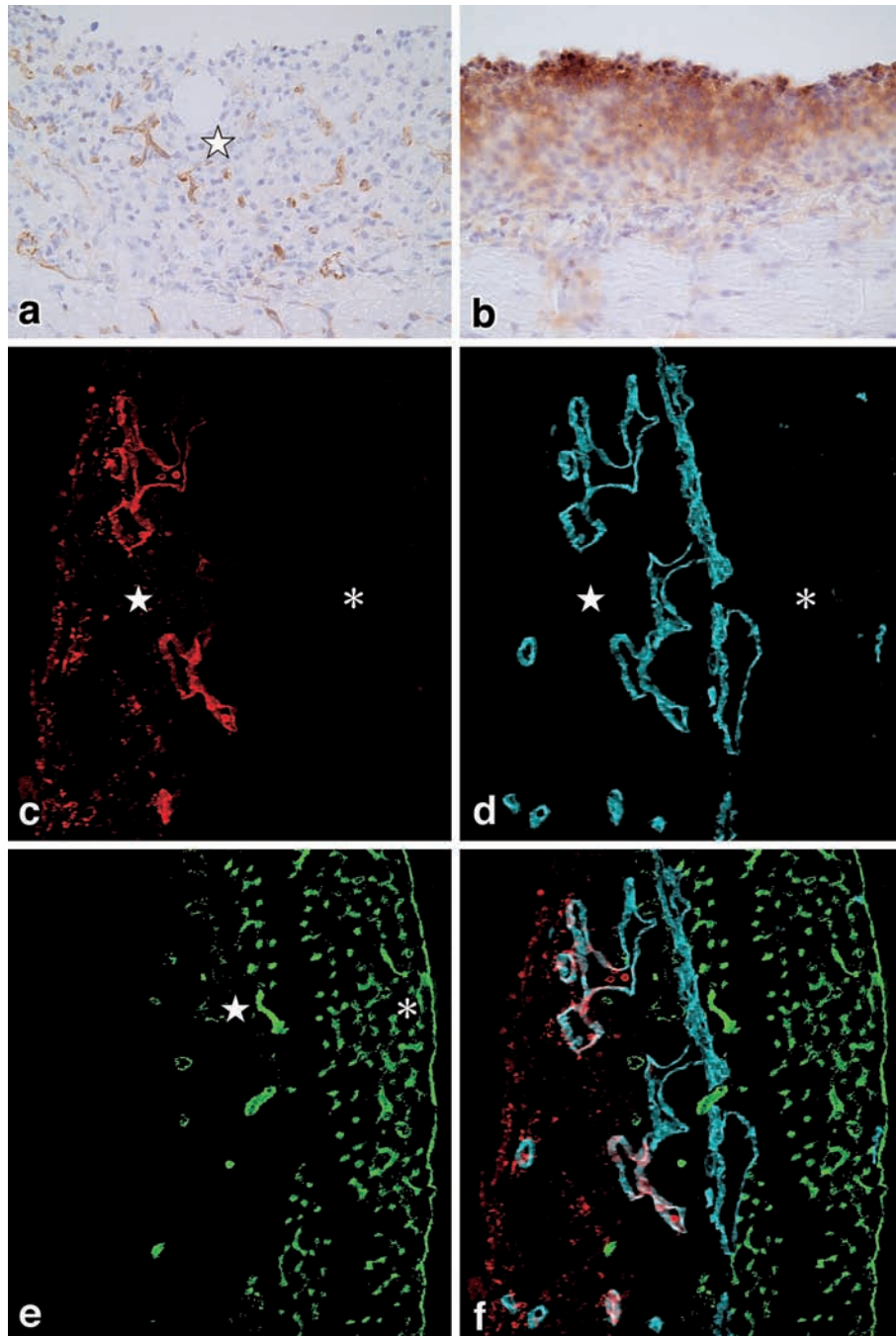
Figure 13 Development of functional vascular structures in lymphangiomas.

Functional vascular structures were detected 28 days after FIA injection in C57BL/6 female mice. Ten-micron thick cryosections were made and immunostained with CD31 **(a)**, vasohibin-2 (VASH2), a tumor angiogenesis promoting factor **(b)**.

In **c-f,** blood vessels were labed by intravenous injection with FITC-conjugated tomato lectin (LEL), the mice were then perfusion-fixed with 4% PFA for 10 min, washed and frozen in OCT compound. Ten-micron thick cryosections were made and immunostained. Triple fluorescent staining with LA102 (c), LYVE-1 (d), and tomato LEL lectin (e). The merged image (f). All blood vessels that have blood supply are strongly stained by the FITC-LEL (e). Note that LYVE-1+ lymphatic vessels extend from the borders between the diaphragm (✱) and lymphangioma (☆) and formed various shaped lymphatic vessels, while LA102+ vessels mainly exist in lymphangiomas (c, f). Depending on their distribution sites, the positivity of LYVE-1 and LA102 does not necessarily correspond with each other.
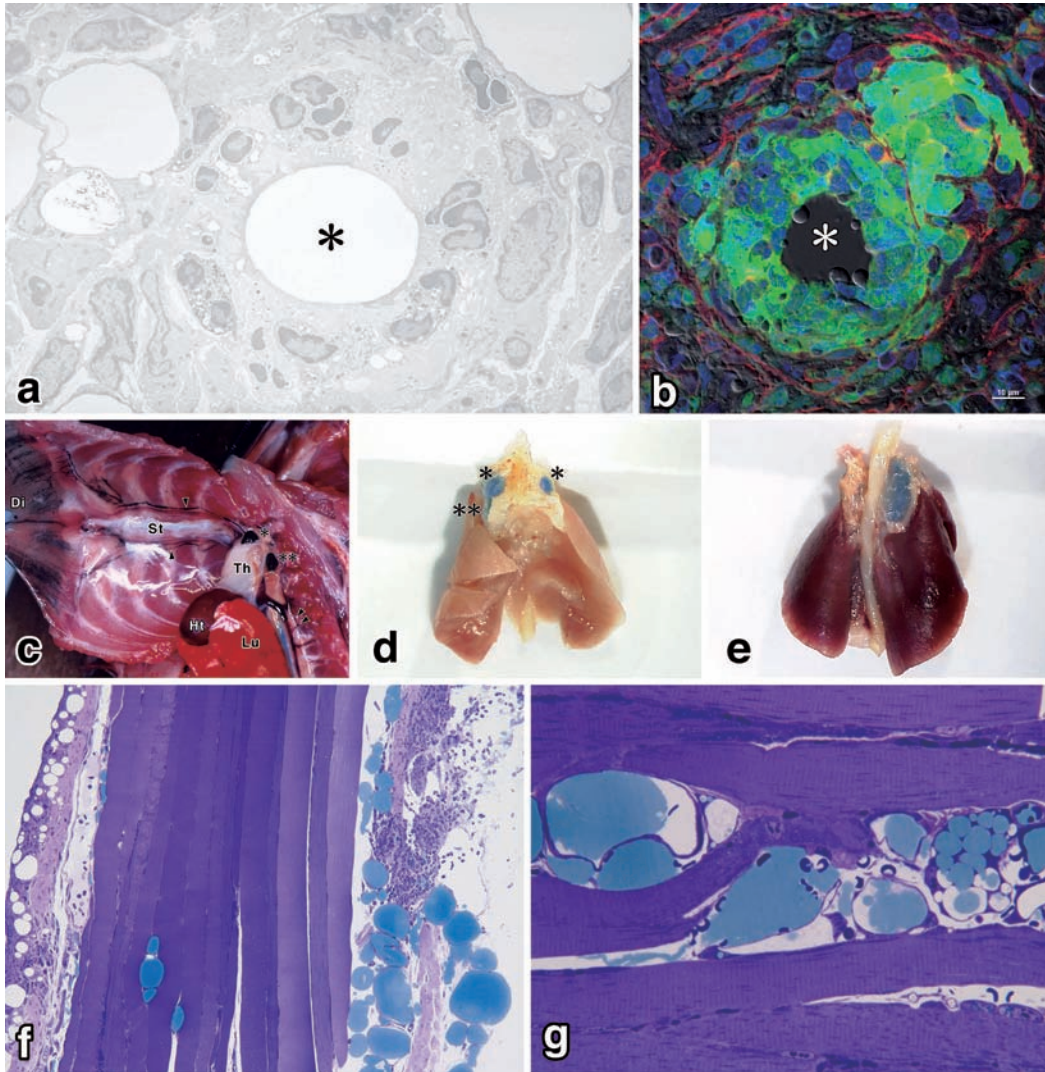
Figure 14 Drainage of FIA out of peritoneal cavity via the newly formed functional lymphatics.

a: Transmission electron micrograph of a typical fat-storing follicular structure (＊) on day 28 of FIA injection. **b:** A confocal triple immunofluorescent image of follicular structure similar to that shown in (a) on day 28 of FIA injection. Chimeric large cell masses containing GFP^{+} bone marrow-derived cells (green), podoplanin^{+} mesothelial cells (red), and CD68^{+} macrophages (blue). Note that various sizes of fat droplets were incorporated and some were secreted inside the follicle (＊).

c: The two main routes of lymphatic pathways from abdominal cavity in the normal control animal. Carbon dyes injected intraperitoneally were absorbed from the diaphragm and transported into the thoracic cavity by lymphatic vessels. A main route is parasternal or anterior route (arrow heads), reaching the regional parathymic lymph nodes (＊). The other is the dorsal or posterior route (double arrowheads), reaching the posterior mediastinal lymph nodes (＊＊). Di: diaphragm, Ht: heart, Lu: lung, St: sterna, Th: thymus. **d:** FIA (with EM blue) reached the parathymic lymph nodes (＊) and the posterior mediastinal lymph nodes (＊＊) within seven days after intraperitoneal injection. **e:** FIA (with EM blue) reached parathymic or posterior mediastinal lymph nodes more than four months after intraperitoneal injection. Note that these regional lymph nodes swelled and fused together at the late stages of tumor development.

f: Formation of abnormal intermuscular draining routes from the peritoneal cavity (on the left) towards the subcutis in the abdominal skin (on the right). **g:** Higher magnification view of the abnormal intermuscular draining routes of FIA. Note that various-sized fat droplets or even whole fat-storing cells are transported in the tubular structures as shown in Figure 9f&g.
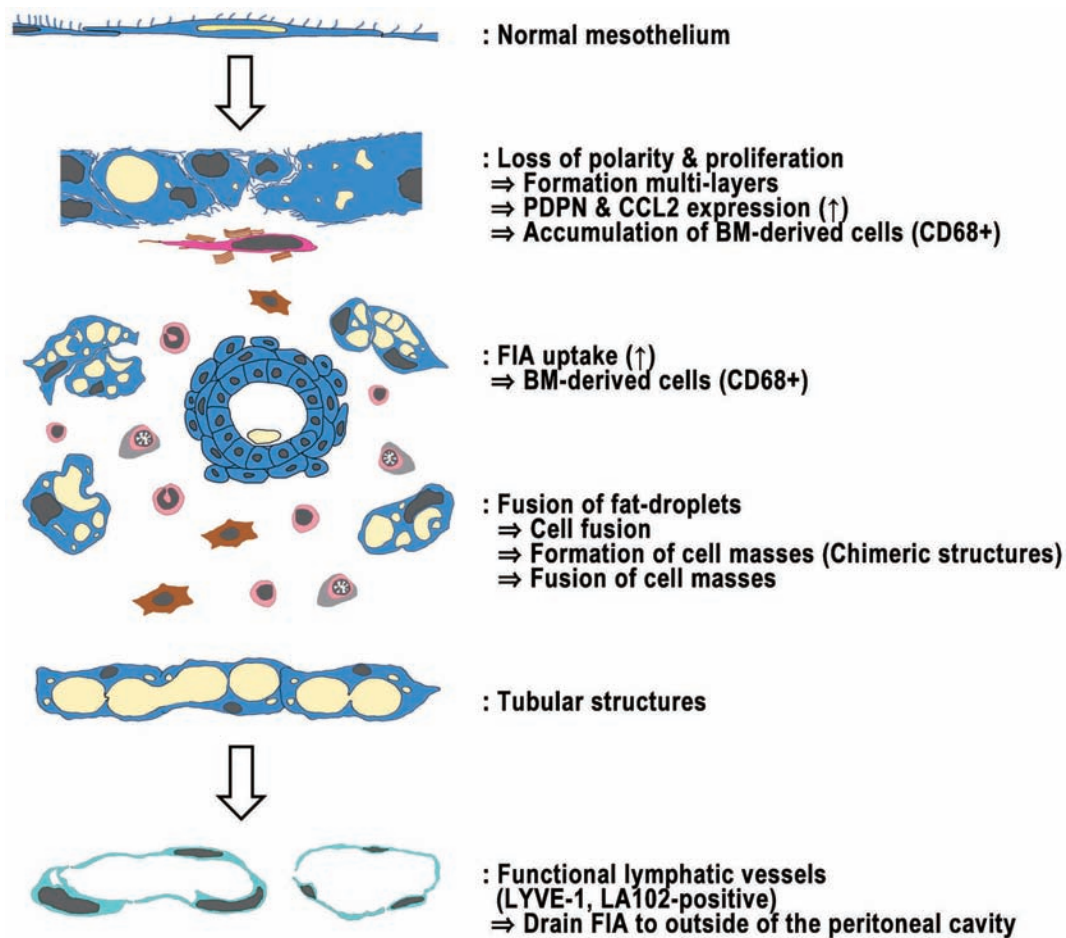
Figure 15 Hypothesis: mesothelial-endothelial transformation.
The possible processes and mechanisms involved in the development of FIA-induced lymphangiomas. Sequential changes from mesothelial cells to lymphatic endothelial cells via various fat-storing lymphangioma cells are suggested. These phenomena may be interpreted as one of the biological defense mechanisms to drain extrinsic adjuvant oil out of the peritoneal cavity.

mor model. We found the podoplanin⁺ cells induced a chemokine CCL2 to recruit CD68⁺ bone marrow-derived cells which accumulated from the peritoneal cavity.[74] Both M1 and M2 type macrophages might be involved in the early stage of tumor development. Macrophages are responsible for adipose tissue remodeling[96] and various pathological conditions, such as atherosclerosis.[87,88] It has also been reported that the vast majority of macrophages infiltrating the obese organ are arranged around dead adipocytes, forming characteristic crown-like structures (CLS).[97] The large follicular structures consisting of podoplanin⁺ mesothelial cells and CD68⁺ macrophages in our tumor model **(Figure 14a&b)** may be very close or almost equivalent to CLS. Furthermore, Detry et. al.[98] also suggested the possibil-

ity that FIA-induced lymphangiomas formed tubular structures, like lymphatic vessels.

The results demonstrated in this study suggest sequential changes from mesothelial cells to lymphatic endothelial cells via fat-storing lymphangioma cells after FIA stimulations. These phenomena may be interpreted as one of the biological defense mechanisms to drain extrinsic adjuvant oil out of the peritoneal cavity. We have suggested the possibility of sequential transformation **(Figure 15)** from peritoneal mesothelial cells to functional lymphatic vessels via fat-storing tumor cells after FIA stimulation.[74,99] Besides sharing the same mesenchymal origin, both lymphatic endothelial and mesothelial cells have several similarities in their function and structure (as shown in **Figure 2b**). Moreover,

the two cell types might have some ability to transform into various interstitial cells under pathological conditions or in vitro. However, in vivo, there has been no clear evidence to show the relationship between the two cell types. The biological significance of FIA-induced lymphangiomas and the diversity of mesothelial cells might be important with respect to the relationship between fat cells and lymphatic endothelial cells.

Finally, during our analyses of tumor development in the peritoneal cavity, we observed biased site difference in tumor occurrence. The tumors easily developed almost everywhere, such as the surface of the diaphragm, omentum, liver, spleen, and abdominal wall, except the ovary.[99] The ovarian surface (or germinal) epithelial cells never formed any tumor mass (n ≧ 59 females), although they became strongly positive for podoplanin similar to other peritoneal mesothelial cells forming lymphangiomas at different sites in the peritoneal cavity (unpublished data). These results suggest that the peritoneal mesothelial cells might have diversity in their phenotypic transformation depending on the site of peritoneal cavity. This might be due to the fact that the majority of ovarian tumors derive from the surface (or germinal) epithelial cells and the heterogeneity of the mesothelium in response to FIA.

4. Prospective for the clinical application of this tumor model

The mechanism for lymphangiogenesis is of major interest in both basic and clinical lymphology. It is clear that FIA (or mineral oil) is involved in a high degree of interrelationship between mesothelium and endothelium and is a factor that bring these two structures closer. This process has recently gained considerable attention, and studies to understand this process are important for explaining the mechanism of lymphangiogenesis.[100] If the shift between mesothelial and lymphatic endothelial cells can be controlled, it might be possible to develop treatment for chronic lymphedema and even peritoneal sclerosis in patients on peritoneal dialysis. The hypothesis **(Figure 15)** might give some hints for the possible application of peritoneal dialysis or the treatment of chronic edemas.

Conclusions

The one of the important missions of lymphatic vessels is to absorb fat as well as macromolecules and lymphoid cells and transport them into the systemic blood circulation. Once the lymphatic vessel function is disturbed under various abnormal conditions, some biological defense mechanisms recover the draining capacity by involving various cell types, such as mesothelial cells and fat droplet containing macrophages. Therefore, adjuvant-induced lymphangiomas would provide us useful experimental animal models to clarify some of the unanswered aspects [17] in the lymphatic system under both normal and pathological conditions.

Conflicts of Interest: There are no conflicts of interest to declare.

References

1. Rosai J, Levine GD: Tumors of the thymus. *In* Atlas of tumor pathology, 2nd series, fasc.13, pp34−161, Armed Forces Institute of Pathology, Washington,

D.C. (1976)

2. Ezaki T, Marbrook J: The haemolytic plaque reduction technique to measure cytotoxicity with hybridoma cells as a target. J Immunol Methods 54: 281–290, 1982

3. Ezaki T, Skinner MA, Marbrook J: Spontaneous cytotoxic T cells in murine spleen-cell cultures. I. Some characteristics of effector and precursor cells. Immunology 50: 343–349, 1983

4. Ezaki T, Skinner MA, Marbrook J: Spontaneous cytotoxic T cells in murine spleen-cell cultures. II. Distinguishing between spontaneous cytotoxic T cells and NK cells according to kinetics and target selectivity. Immunology 50: 351–357, 1983

5. Ezaki T, Marbrook J: The use of hybridoma cells as a murine model to study tumor immunity. Int J Cancer 35: 107–111, 1985

6. Skinner MA, Thompson K, Ezaki T et al: Effects of in vivo modulation of splenic natural killer cell activity on the growth of spleen-seeking tumour variants. Br J Cancer 55: 259–263, 1987

7. Ezaki T, Kawatsu R, Matsuno K et al: Characterization of intrathymic and extrathymic T cell development in spontaneous thymoma Buffalo/Mna rats. Thymus 16: 67–87, 1990

8. Ezaki T, Matsuno K, Kotani M: Unique thymic microenvironment for T-cell development in spontaneous thymoma BUF/Mna rats. *In* Lymphatic tissues and in vivo immune responses (Imhof BA, Berrih-Aknin S, Ezine S eds), pp105–109, Marcel Dekker, New York (1991)

9. Ezaki T, Matsuno K, Kotani M: Thymic nurse cells (TNC) in spontaneous thymoma BUF/Mna rats as a model to study their roles in T-cell development. Immunology 73: 151–158, 1991

10. Ezaki T, Uehara Y: Thymic nurse cells forming a dynamic microenvironment in spontaneous thymoma BUF/Mna rats. Arch Histol Cytol 60: 39–51, 1997

11. Morikawa S, Baluk P, Kaidoh T et al: Abnormalities in pericytes on blood vessels and endothelial sprouts in tumors. Am J Pathol 160: 985–1000, 2002

12. Baluk P, Morikawa S, Haskell A et al: Abnormalities of basement membrane on blood vessels and endothelial sprouts in tumors. Am J Pathol 163: 1801–1815, 2003

13. Kitahara S, Suzuki Y, Morishima M et al: Vasohibin-2 modulates tumor onset in the gastrointestinal tract by normalizing tumor angiogenesis. Mol Cancer 13: 99, 2014

14. Ezaki T: How can we detect lymphatic vessels? Japanese Journal of Lymphology 35: 105–107, 2012 (in Japanese)

15. Kotani M, Nawa Y, Fujii H et al: Post-capillary venules as the pathway for migrating B lymphocytes. Cell Tissue Res 152: 299–303, 1974

16. Ezaki T, Matsuno K, Fujii H et al: Characterization of rat vascular endothelial cell antigens by monoclonal antibodies. Acta Anatomica Nipponica 64: 390, 1989

17. Ezaki T, Kotani M: Mysteries in lymph, lymphatics, and lymphoid tissues. J Tokyo Wom Med Univ 89 (Extra 1): E4–E65, 2019

18. Ezaki T, Matsuno K, Fujii H et al: A new approach for identification of rat lymphatic capillaries using a monoclonal antibody. Arch Histol Cytol 53 (Suppl): 77–86, 1990

19. Swartz MA, Skobe M: Lymphatic function, lymphangiogenesis, and cancer metastasis. Microsc Res Tech 55: 92–99, 2001

20. Scavelli C, Weber E, Agliano M et al: Lymphatics at the crossroads of angiogenesis and lymphangiogenesis. J Anat 204: 433–449, 2004

21. Baluk P, Tammela T, Ator E et al: Pathogenesis of persistent lymphatic vessel hyperplasia in chronic airway inflammation. J Clin Invest 115: 247–257, 2005

22. Tammela T, Petrova TV, Alitalo K: Molecular lymphangiogenesis: new players. Trends Cell Biol 15: 434–441, 2005

23. Hirakawa S, Hong YK, Harvey N et al: Identification of vascular lineage-specific genes by transcriptional profiling of isolated blood vascular and lymphatic endothelial cells. Am J Pathol 162: 575–586, 2003

24. Banerji S, Ni J, Wang SX et al: LYVE-1, a new homologue of the CD44 glycoprotein, is a lymph-specific receptor for hyaluronan. J Cell Biol 144: 789–801, 1999

25. Breiteneder-Geleff S, Soleiman A, Kowalski H et al: Angiosarcomas express mixed endothelial phenotypes of blood and lymphatic capillaries: podoplanin as a specific marker for lymphatic endothelium. Am J Pathol 154: 385–394, 1999

26. Schacht V, Dadras SS, Johnson LA et al: Up-regulation of the lymphatic marker podoplanin, a mucin-type transmembrane glycoprotein, in human squamous cell carcinomas and germ cell tumors. Am J Pathol 166: 913–921, 2005

27. Wigle JT, Oliver G: Prox1 function is required for the development of the murine lymphatic system. Cell 98: 769–778, 1999

28. Partanen TA, Alitalo K, Miettinen M: Lack of lymphatic vascular specificity of vascular endothelial growth factor receptor 3 in 185 vascular tumors. Cancer 86: 2406–2412, 1999

29. Mouta Carreira C, Nasser SM, di Tomaso E et al: LYVE-1 is not restricted to the lymph vessels: expression in normal liver blood sinusoids and down-regulation in human liver cancer and cirrhosis. Cancer Res 61: 8079–8084, 2001

30. Jackson DG, Prevo R, Clasper S et al: LYVE-1, the lymphatic system and tumor lymphangiogenesis. Trends Immunol 22: 317–321, 2001

31. Mancardi S, Stanta G, Dusetti N et al: Lymphatic endothelial tumors induced by intraperitoneal injection of incomplete Freund's adjuvant. Exp Cell Res 246: 368–375, 1999

32. Ezaki T, Kuwahara K, Morikawa S et al: Characterization of adjuvant-induced rat lymphangiomas as a model to study the lymph drainage from abdominal cavity. Japanese Journal of Lymphology 27: 1–10, 2004

33. Toshimori K, Araki S, Oura C: Masking of sperm maturation antigen by sialic acid in the epididymis of the mouse. An immunohistochemical study. His-

tochemistry 90: 195–200, 1988

34. Ezaki T, Kuwahara K, Morikawa S et al: Production of two novel monoclonal antibodies that distinguish mouse lymphatic and blood vascular endothelial cells. Anat Embryol (Berl) 211: 379–393, 2006

35. Ezaki T, Baluk P, Thurston G et al: Time course of endothelial cell proliferation and microvascular remodeling in chronic inflammation. Am J Pathol 158: 2043–2055, 2001

36. Sironi M, Conti A, Bernasconi S et al: Generation and characterization of a mouse lymphatic endothelial cell line. Cell Tissue Res 325: 91–100, 2006

37. Low MG, Kincade PW: Phosphatidylinositol is the membrane-anchoring domain of the Thy-1 glycoprotein. Nature 318: 62–64, 1985

38. Jurisic G, Iolyeva M, Proulx ST et al: Thymus cell antigen 1 (Thy1, CD90) is expressed by lymphatic vessels and mediates cell adhesion to lymphatic endothelium. Exp Cell Res 316: 2982–2992, 2010

39. Crawford JM, Barton RW: Thy-1 glycoprotein: structure, distribution, and ontogeny. Lab Invest 54: 122–135, 1986

40. Reif AE, Allen JM: Immunological distinction of AKR thymocytes. Nature 203: 886–887, 1964

41. Kroczek RA, Gunter KC, Germain RN et al: Thy-1 functions as a signal transduction molecule in T lymphocytes and transfected B lymphocytes. Nature 322: 181–184, 1986

42. Williams AF: Many cells in rat bone marrow have cell-surface Thy-1 antigen. Eur J Immunol 6: 526–528, 1976

43. Williams AF, Barclay AN, Letarte-Muirhead M et al: Rat thy-1 antigens from thymus and brain: their tissue distribution, purification, and chemical composition. Cold Spring Harb Symp Quant Biol 41 Pt 1: 51–61, 1977

44. Pont S, Regnier-Vigouroux A, Marchetto S et al: A Thy-1.1-specific monoclonal alloantibody activates both mouse and rat T cells. Cell Immunol 107: 64–73, 1987

45. Ishizu A, Ishikura H, Nakamaru Y et al: Interleukin-1 alpha regulates Thy-1 expression on rat vascular endothelial cells. Microvasc Res 53: 73–78, 1997

46. Saalbach A, Haustein UF, Anderegg U: A ligand of human thy-1 is localized on polymorphonuclear leukocytes and monocytes and mediates the binding to activated thy-1-positive microvascular endothelial cells and fibroblasts. J Invest Dermatol 115: 882–888, 2000

47. Saalbach A, Wetzig T, Haustein UF et al: Detection of human soluble Thy-1 in serum by ELISA. Fibroblasts and activated endothelial cells are a possible source of soluble Thy-1 in serum. Cell Tissue Res 298: 307–315, 1999

48. Dalchau R, Daar AS, Fabre JW: The human Thy-1 molecule. Immunol Ser 45: 185–196, 1989

49. Reif AE, Allen JM: The AKR thymic antigen and its distribution in leukemias and nervous tissues. J Exp Med 120: 413–433, 1964

50. Williams AF, Gagnon J: Neuronal cell Thy-1 glycoprotein: homology with immunoglobulin. Science 216: 696–703, 1982

51. Ezaki T: Progress in imaging of lymphatic vessels and its prospects. The Cell 47: 622–624, 2015 (in Japanese)

52. Thurston G, Baluk P, Hirata A et al: Permeability-related changes revealed at endothelial cell borders in inflamed venules by lectin binding. Am J Physiol 271: H2547–H2562, 1996

53. Nakamura-Ishizu A, Morikawa S, Shimizu K et al: Characterization of sinusoidal endothelial cells of the liver and bone marrow using an intravital lectin injection method. J Mol Histol 39: 471–479, 2008

54. Tatsuzuki A, Ezaki T, Makino Y et al: Characterization of the sugar chain expression of normal term human placental villi using lectin histochemistry combined with immunohistochemistry. Arch Histol Cytol 72: 35–49, 2009

55. Morikawa S, Shimizu K, Ezaki T: Comparative analyses of sugar chain expression on the endothelium between lymphatic vessels and blood vessels to characterize the function of sugar residues on the lymphatic endothelium. Inflammation & Immunity 24 (5): 385–390, 2016 (in Japanese)

56. Yaniv K, Isogai S, Castranova D et al: Live imaging of lymphatic development in the zebrafish. Nat Med 12: 711–716, 2006

57. Isogai S, Hitomi J, Yaniv K et al: Zebrafish as a new animal model to study lymphangiogenesis. Anat Sci Int 84: 102–111, 2009

58. Ogata F, Azuma R, Kikuchi M et al: Novel lymphography using indocyanine green dye for near-infrared fluorescence labeling. Ann Plast Surg 58: 652–655, 2007

59. Morton DL, Wen DR, Wong JH et al: Technical details of intraoperative lymphatic mapping for early stage melanoma. Arch Surg 127: 392–399, 1992

60. Kitagawa Y, Fujii H, Kumai K et al: Recent advances in sentinel node navigation for gastric cancer: a paradigm shift of surgical management. J Surg Oncol 90: 147–151; discussion 151-152, 2005

61. Takeuchi H, Kitagawa Y: New sentinel node mapping technologies for early gastric cancer. Ann Surg Oncol 20: 522–532, 2013

62. Okuda I, Akita K, Irimoto M et al: Magnetic resonance-thracic ductography (MRTD): Advanced magnetic resonance imaging for the lymph vessel and clinical application. The Cell 47: 635–638, 2015 (in Japanese)

63. Kawai Y, Ajima K, Nagai T et al: Real-time imaging of the lymphatic channels and sentinel lymph nodes of the stomach using contrast-enhanced ultrasonography with Sonazoid in a porcine model. Cancer Sci 102: 2073–2081, 2011

64. Yoffey JM, Courtice FC: Lymphatics, lymph and lymphoid tissue, 2nd ed, Edward Arnold (Publishers), London (1956)

65. Rusznyák I, Földi M, Szabó G: Lymphatics and lymph circulation: physiology and pathology, Pergamon Press, Oxford, New York (1960)

66. Yoffey JM, Courtice FC: Lymph flow from regional lymphatics. Section XV: The pleural and peritoneal cavities. *In* Lymphatics, lymph and the lymphomyeloid complex (Yoffey JM, Courtice FC eds), pp295–309, Academic Press, New York (1970)

67. Habu K: Studies on the distribution of lymphatic vessels in the diaphragm and absorption of carbon particles from the peritoneal cavity in to these vessels. J Kumamoto Med Soc 45: 964−984, 1971 (in Japanese)
68. Abu-Hijleh MF, Habbal OA, Moqattash ST: The role of the diaphragm in lymphatic absorption from the peritoneal cavity. J Anat 186 (Pt 3): 453−467, 1995
69. Fritz DL, Waag DM: Transdiaphragmatic lymphatic transport of intraperitoneally administered marker in hamsters. Lab Anim Sci 49: 522−529, 1999
70. Bettendorf U: Lymph flow mechanism of the subperitoneal diaphragmatic lymphatics. Lymphology 11: 111−116, 1978
71. Bettendorf U: Electronmicroscopic studies on the peritoneal resorption of intraperitoneally injected latex particles via the diaphragmatic lymphatics. Lymphology 12: 66−70, 1979
72. Yuan Z, Rodela H, Hay JB et al: Lymph flow and lymphatic drainage of inflammatory cells from the peritoneal cavity in a casein-peritonitis model in sheep. Lymphology 27: 114−128, 1994
73. Ezaki T, Desaki J: Lymphangiogenic responses in an adjuvant-induced lymphangioma model. Japanese Journal of Lymphology 35: 14−17, 2012 (in Japanese)
74. Ezaki T, Shimizu K, Sedohara A et al: Mechanisms for tumorigenesis in an adjuvant-induced lymphangioma model in mice. Japanese Journal of Lymphology 41: 102−106, 2018 (in Japanese)
75. Kato S, Miyauchi R: Enzyme-histochemical visualization of lymphatic capillaries in the mouse tongue: light and electron microscopic study. Okajimas Folia Anat Jpn 65: 391−403, 1989
76. Leak LV, Potter M, Mayfield WJ: Response of the peritoneal mesothelium to the mineral oil, pristane. Curr Top Microbiol Immunol 122: 221−233, 1985
77. Morton H: Early pregnancy factor: an extracellular chaperonin 10 homologue. Immunol Cell Biol 76: 483−496, 1998
78. Quinn KA: Active immunization with EPF suppresses the formation of immune ascites in BALB/c mice. Immunol Cell Biol 69 (Pt 1): 1−6, 1991
79. Potter M, Boyce CR: Induction of plasma-cell neoplasms in strain BALB/c mice with mineral oil and mineral oil adjuvants. Nature 193: 1086−1087, 1962
80. Potter M, Maccardle RC: Histology of developing plasma cell neoplasia induced by mineral oil in Balb/c mice. J Natl Cancer Inst 33: 497−515, 1964
81. Gordon S, Plüddemann A, Martinez Estrada F: Macrophage heterogeneity in tissues: phenotypic diversity and functions. Immunol Rev 262: 36−55, 2014
82. Torres A, Makowski L, Wellen KE: Immunometabolism: metabolism fine-tunes macrophage activation. Elife 5: e14354, 2016
83. Shimizu K, Arimura Y, Ezaki T: Roles of podoplanin positive cells in wound healing of the mouse tongue. FASEB J 29 (1_supplement): Abstract Number 346.5, 2015
84. Shimizu K, Ezaki T: Podoplanin positive stromal cells guide CD68 positive cells by forming an extravascular pathway in wound healing of the mouse tongue. Angiogenesis 17 (5th International meeting on angiogenesis): 766−767, 2014
85. Zhao X, Gao M, He J et al: Perilipin1 deficiency in whole body or bone marrow-derived cells attenuates lesions in atherosclerosis-prone mice. PLoS One 10: e0123738, 2015
86. Agardh HE, Folkersen L, Ekstrand J et al: Expression of fatty acid-binding protein 4/aP2 is correlated with plaque instability in carotid atherosclerosis. J Intern Med 269: 200−210, 2011
87. Buers I, Hofnagel O, Ruebel A et al: Lipid droplet associated proteins: an emerging role in atherogenesis. Histol Histopathol 26: 631−642, 2011
88. Yuan Y, Li P, Ye J: Lipid homeostasis and the formation of macrophage-derived foam cells in atherosclerosis. Protein Cell 3: 173−181, 2012
89. Boord JB, Fazio S, Linton MF: Cytoplasmic fatty acid-binding proteins: emerging roles in metabolism and atherosclerosis. Curr Opin Lipidol 13: 141−147, 2002
90. Linton MF, Fazio S: Macrophages, inflammation, and atherosclerosis. Int J Obes Relat Metab Disord 27 Suppl 3: S35−S40, 2003
91. Owada Y, Abdelwahab SA, Kitanaka N et al: Altered emotional behavioral responses in mice lacking brain-type fatty acid-binding protein gene. Eur J Neurosci 24: 175−187, 2006
92. Sato Y: The vasohibin family: a novel family for angiogenesis regulation. J Biochem 153: 5−11, 2013
93. Norita R, Suzuki Y, Furutani Y et al: Vasohibin-2 is required for epithelial-mesenchymal transition of ovarian cancer cells by modulating transforming growth factor-β signaling. Cancer Sci 108: 419−426, 2017
94. Navarro-Núñez L, Langan SA, Nash GB et al: The physiological and pathophysiological roles of platelet CLEC-2. Thromb Haemost 109: 991−998, 2013
95. Uhrin P, Zaujec J, Breuss JM et al: Novel function for blood platelets and podoplanin in developmental separation of blood and lymphatic circulation. Blood 115: 3997−4005, 2010
96. Suganami T, Ogawa Y: Adipose tissue macrophages: their role in adipose tissue remodeling. J Leukoc Biol 88: 33−39, 2010
97. Cinti S: Transdifferentiation properties of adipocytes in the adipose organ. Am J Physiol Endocrinol Metab 297: E977−E986, 2009
98. Detry B, Bruyère F, Erpicum C et al: Digging deeper into lymphatic vessel formation in vitro and in vivo. BMC Cell Biol 12: 29, 2011
99. Ezaki T, Nakada K, Sagawa H: Diversity of the peritoneal mesothelial cells: (2) Germinal epithelial cells of the ovary in mice. Experimental Biology 2015, 2015. https://experimentalbiology.org/2015.aspx (Accessed Apr 15, 2019)
100. Rockson SG: Laboratory models for the investigation of lymphangiomatosis. Microvasc Res 96: 64−67, 2014

アジュバント誘導性マウスリンパ管腫の有用性：
リンパ管内皮に関してこの動物モデルから学べること

東京女子医科大学医学部解剖学・発生生物学講座

江﨑　太一

　リンパ管研究はリンパ管内皮細胞に特異的なマーカーの発見と共に急速に進歩した．そこで我々はリンパ管内皮特異的マーカーを発見するために，ネズミでのアジュバント（FIA）誘導性リンパ管腫モデルを用いた．この腫瘍をマウスのリンパ管内皮抗原の供給源として用いることで，LA102 モノクローナル抗体を作製した．この抗体はリンパ管内皮のみを認識し，血管内皮を認識しない．さらに，この抗体の認識する抗原はマウスの CD90.2（Thy-1.2）とホモログであることが分かった．また，LA102 はじめ，その他の内皮細胞に特異的な抗体やレクチンを用いて，リンパ管と血管を三次元的に識別して画像化する方法を開発した．次に，この腫瘍を腹腔中皮細胞とリンパ管内皮との関係を研究するためのモデルとして用いた．FIA を腹腔内投与後 3 日目で，単層扁平な中皮細胞が立方化し，細胞間が解離して極性を失い，さらには多層化した．同時にポドプラニンおよび CCL2 の発現が増加することで骨髄由来の CD68 陽性マクロファージを呼び寄せ，FIA を取り込みながらがリンパ管腫の中に集積していた．リンパ管腫内では次第に，色々な大きさの脂肪滴（FIA）が細胞内で融合し，さらには細胞同士も融合して，巨大化した脂肪摂取細胞がキメラ状の細胞集塊や濾胞様の構造を形成した．つまりこれらの構造は，ポドプラニン陽性の中皮細胞のみならず，骨髄由来のマクロファージ，および間質の間葉系細胞などが集積してリンパ管腫を形成することが分かった．4 週以降になると，これらの細胞集塊は腹腔から脂肪を排導するために管状につながり，機能的なリンパ管構造を形成した．以上から，この一連の中皮細胞から脂肪摂取リンパ管腫を介してのリンパ管内皮細胞への変化は FIA を腹腔から排導するための生体防御反応の一つであると考えられ，脂肪摂取リンパ管腫を介する中皮―内皮間形質転換の可能性を示唆している．

———————————